PREPRINTS

OF THE

STEWARD OBSERVATORY

THE UNIVERSITY OF ARIZONA
TUCSON, ARIZONA

NO. 16

THREE-COLOR PHOTOMETRY OF SOUTHERN QSO:s, RADIO GALAXIES AND NORMAL GALAXIES

B. E. Westerlund and J. V. Wall

December 1968

THREE-COLOR PHOTOMETRY OF SOUTHERN QSO:s, RADIO GALAXIES AND NORMAL GALAXIES

by

B. E. Westerlund and J. V. Wall

Steward Observatory
University of Arizona
Tucson, Arizona

Mount Stromlo and Siding Spring Observatories,
Australian National University, Canberra, Australia

December 1968

THREE-COLOR PHOTOMETRY OF SOUTHERN QSO:s, RADIO GALAXIES AND NORMAL GALAXIES

B. E. Westerlund

Steward Observatory, University of Arizona, Tucson, Arizona

and

J. V. Wall

Mount Stromlo and Siding Spring Observatories,

Australian National University, Canberra, Australia

ABSTRACT

Data on the UBV system are presented for 14 quasistellar radio sources, 8 N galaxies, 39 radio galaxies and 19 radioquiet galaxies south of $+20^{o}$ declination. Their positions in the two-color diagram show that the integrated colors of the radio galaxies are similar to those of the radioquiet galaxies of the same morphological type. In an absolute radio magnitude - radio index diagram a linear relation exists between M_{158} and $(m_{158} - B)_o$ for radio galaxies of all classes. The QSO:s, however, do not follow this relation, and possible explanations are considered.

The brightness and color distributions in the larger galaxies are described in detail. Our results are combined with other data for a discussion of the compositions of these systems. It is suggested that a fairly high amount of reddening occurs in the central regions of several galaxies, as for instance, in NGC 1068 and NGC 1316.

I. INTRODUCTION

Most of the recent discussions of optical features of radio sources have, quite understandably, been centered on the QSO:s, the N Galaxies and the possibly related Seyfert galaxies. It seems, however, essential that for an improved understanding of the physics of the strong as well as of the weak radio emitters a statistically significant material of photométric and spectroscopic data should be gathered. The present paper gives photometric data for 80 objects south of $+20^{\circ}$ declination; 19 are radio quiet galaxies and 14 are QSO:s. For a number of these objects new radial velocity data are given; they are determined by Westerlund and Stokes (1968). Progress reports on the present investigation have been presented by Westerlund, Wall and Stokes (1967) and by Westerlund and Wall (1968).

Originally, the aims of the investigation were 1) to confirm the classification of the QSO:s and the N galaxies and 2) to compare the radio galaxies with the radioquiet galaxies by means of the integrated colors. However, the available data, including the new velocity determinations, permit also a study of the dependence of the absolute radio intensity, on the radio index. Furthermore, we will show that for the galaxies observed with a series of apertures, both the surface brightness distributions and the color variations with the distance from the center give important information about the composition of these galaxies.

II. THE OBSERVATIONS

The radio sources observed in the present investigation are listed in the Parkes catalogue of radio sources (Bolton et al 1964; Price and Milne 1965; Day et al 1966; Shimmins et al 1966). The identidications have been made by Bolton et al (1965, 1966a, 1966b, 1966c, 1967); by Westerlund and Smith (1966); and in the case of 1610 - 60 independently by Mills and by Ekers (private communications).

All the Parkes catalogue radio galaxies brighter than $13^{m}.5$, except NGC 253 and NGC 5128, are included in our photometry. The brightest galaxies have been measured with a series of apertures. A number of fainter radio galaxies are also included.

Of the observed radioquiet galaxies 8 were chosen as being close to radio sources. The others either are members of clusters or groups which we are studying or show some optical peculiarities.

All the observations were carried out during 1966 with the 24" and 40" telescopes at Siding Spring Observatory. Dry ice refrigerated 1P21 photomultipliers were used together with the U,B,V, filters recommended by Johnson (1955). Transformations from the instrumental to the standard U,B,V system were determined for each night using original U,B,V standards, Harvard E-region standards (Westerlund 1963), and stars in IC 4665 (Johnson 1954). Extinction coefficients were likewise determined nightly. All objects fainter than 14th mag were observed with the 40" telescope; off-set techniques were necessary for objects fainter than about V = 15.5 mag.

Most of the QSO:s (Table 1) and half the number of N galaxies (Table 2) were observed during one night, only. The other radio galaxies (Table 3) and the radioquiet galaxies (Table 4) have been observed during two or more nights. Integration times for each aperture and filter were generally taken of sufficient length to give probable errors of about $\pm$0.02 mag in B - V and $\pm$0.04 mag in U - B for objects brighter than V = 14 mag. For the faintest objects the errors are estimated to be about $\pm$0.1 mag.

The observations are presented in Tables 1, 2, 3, and 4. In Tables 1 and 2 the successive columns give:

Col. 1. The Parkes catalogue number.

2. Reference for finding chart.

3. Julian date of observation.

4-6. The U,B,V data.

7. The radio magnitude at 158 Mc/s defined as by (Brown and Hazard 1961).

8-9. The galactic coordinates.

10. Notes.

Table 3 is arranged in a similar way and is self-explanatory. The last column gives 3C or 4C numbers, and an "R" indicates that additional information is given in the Remarks following the Table. Table 4 is, likewise, self-explanatory.

An asterisk at the largest aperture value used for a galaxy in Table 3 indicates that it is less than three times the size of the galaxy on the Palomar Sky Survey plates.

The information in the Remarks to the tables has been taken from

the General Catalogue of Discrete Radio Sources (Howard and Maran 1964) unless otherwise indicated. The classification of the brighter galaxies has been taken from the Reference Catalogue of Bright Galaxies (G. and A. de Vaucouleurs 1964).

The observations of the objects in Tables 1 and 2 were mostly done with an aperture of 18" diameter (a few cases 23").

III. COMPARISONS WITH OTHER OBSERVERS

Tifft (1968b) and de Vaucouleurs (1961) have observed NGC 4374 and NGC 4486 with series of apertures. Their data are compared with ours in Fig. 1; Tifft's results have been reduced to the UBV system following de Vaucouleurs' equations (1961).

We conclude that the agreement is satisfactory between Tifft's and our observations. The values in de Vaucouleurs' catalogue are a few hundreds of a magnitude bluer than ours. The discrepancies in U - B in the nuclear region of NGC 4486 may be due to a real variation with time (Cf. Tifft 1968b), but it may also simply reveal the well known difficulties encountered in photometry of the nuclei of galaxies, here enhanced by the existence of the jet.

NGC 1068 has been observed photoelectrically by Sandage (1967b) and by Chincarini (Walker 1968) with a series of apertures. The integrated colors are compared in Fig. 2 as functions of the diameters of the apertures. With the exception of two points where Chincarini's colors are appreciably redder than ours, the agreement is quite good. It is again possible that the slight differences in aperture sizes

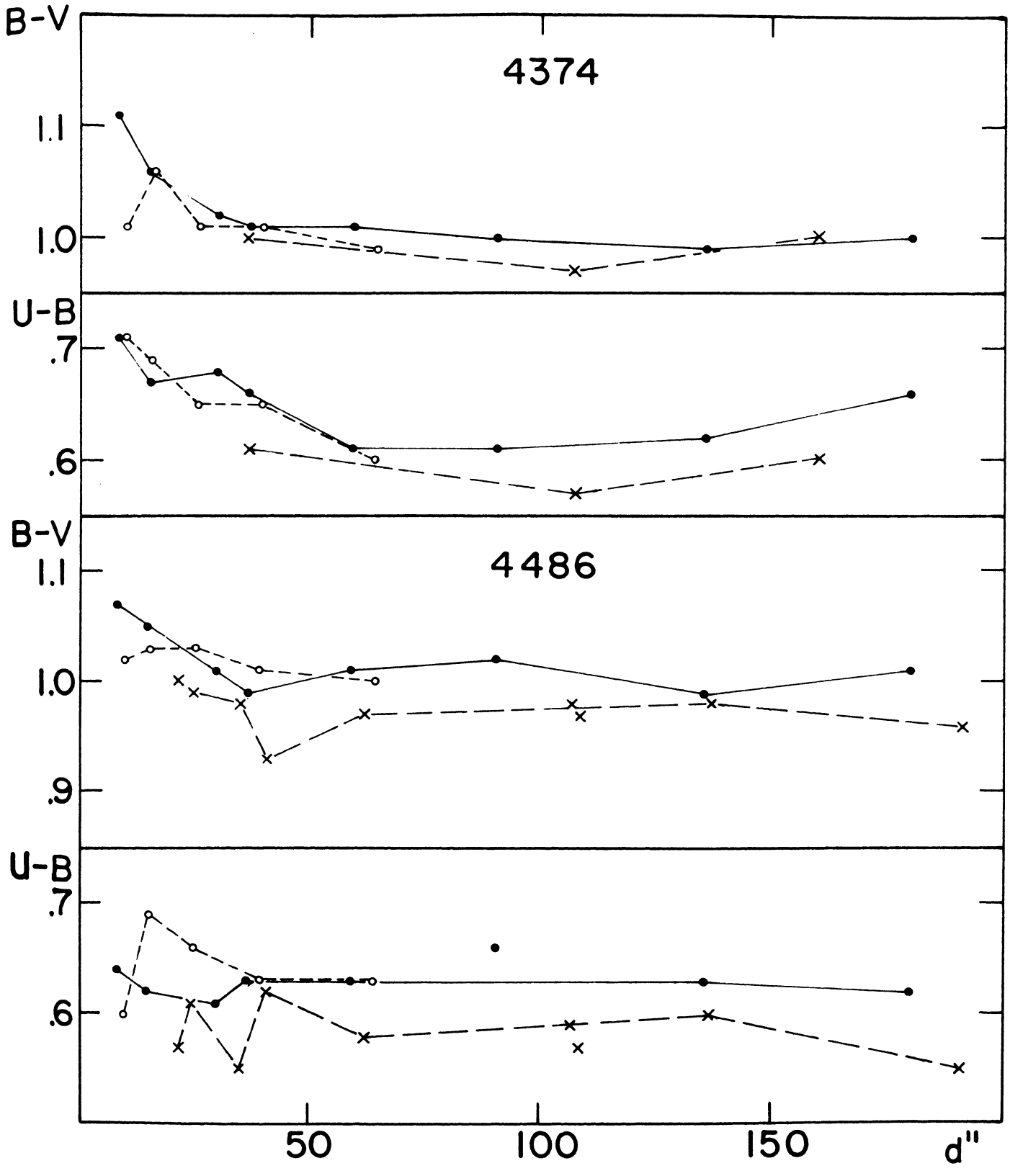

Fig. 1 Comparison of multi-aperture observations of NGC 4374 and NGC 4486. Observations by us are plotted as dots, by Tifft as open circles, and by de Vaucouleurs as x.

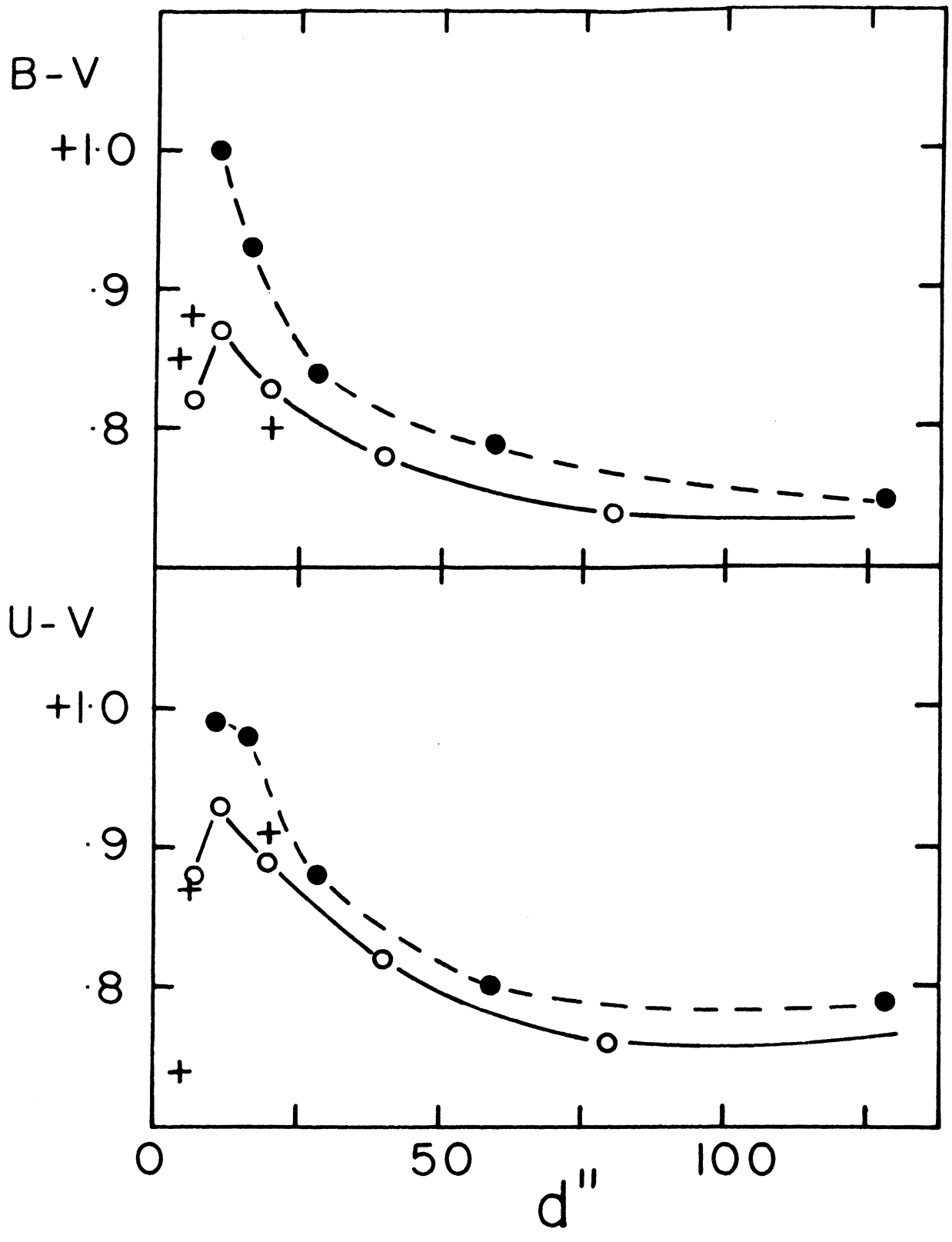

Fig. 2 Comparison of multi-aperture observations of NGC 1068. Observations by us are plotted as dots, by Sandage as +, and by Chincarini as open circles.

contribute to this effect. It is of course also possible that the nucleus of NGC 1068 has varied slightly; the observations are obtained at different epochs; but we consider this at present as less likely.

Finally, we compare in Fig. 3 the surface brightness distribution in blue light in NGC 4486 as observed by van Houten (1961), by Markaryan et al (1965), by Tifft (1968b), and by us; and in Fig. 3 the surface brightness distribution in NGC 1068 as observed by van Houten and by us. Considering the different techniques used it may be concluded that the agreement is good.

IV. THE TWO-COLOR DIAGRAM

We have applied corrections for galactic absorption on the basis of Shane and Wirtanen's recent investigation (1967). Thus, the total galactic absorption in blue, A_B, has been determined from their Figure 8 wherever possible, and for the remainder of the galaxies the average coefficient P=0.51 mag has been used. The corresponding expression for the colors are $E_{B-V}=0.2\ A_B$ and $E_{U-B} = 0.8E_{B-V}$ for galaxies of "average" colors (Cf. de Vaucouleurs 1961).

The corrected colors are plotted in Fig. 4 for all the observed objects. In most cases the integrated colors are used (=largest aperture). However, for NGC 5236, NGC 7232, NGC 1068, and Fornax A the values for the nuclei (smallest aperture) are plotted, since the nuclei are supposed to be the centers for the radio emission

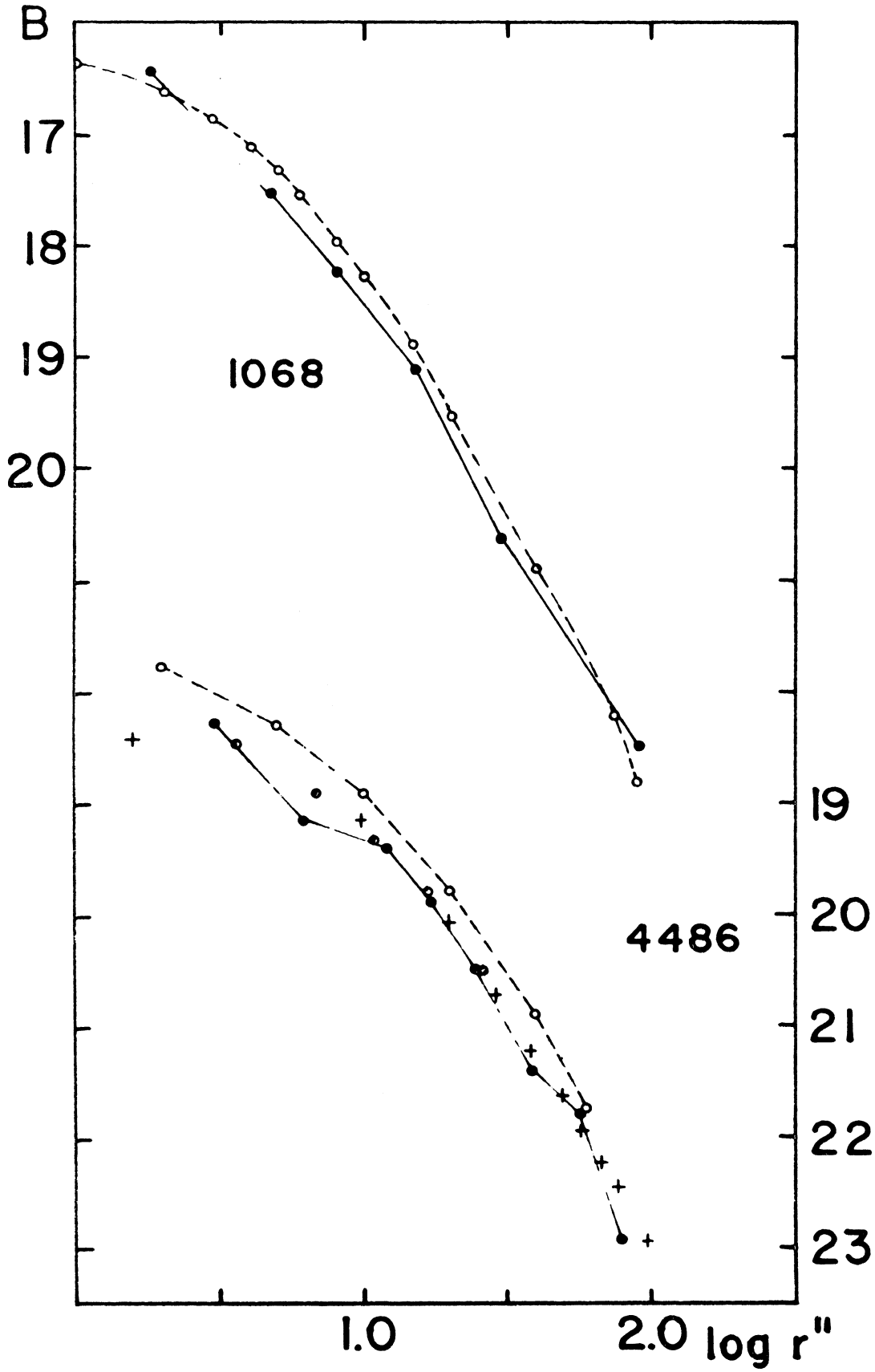

Fig. 3 Comparison of observed surface brightnesses in blue light in NGC 1068 and in NGC 4486. Unit in B is mag/□". Our observations are plotted as dots, van Houten's as open circles, Markaryan et al's as +, and Tifft's as half-filled circles.

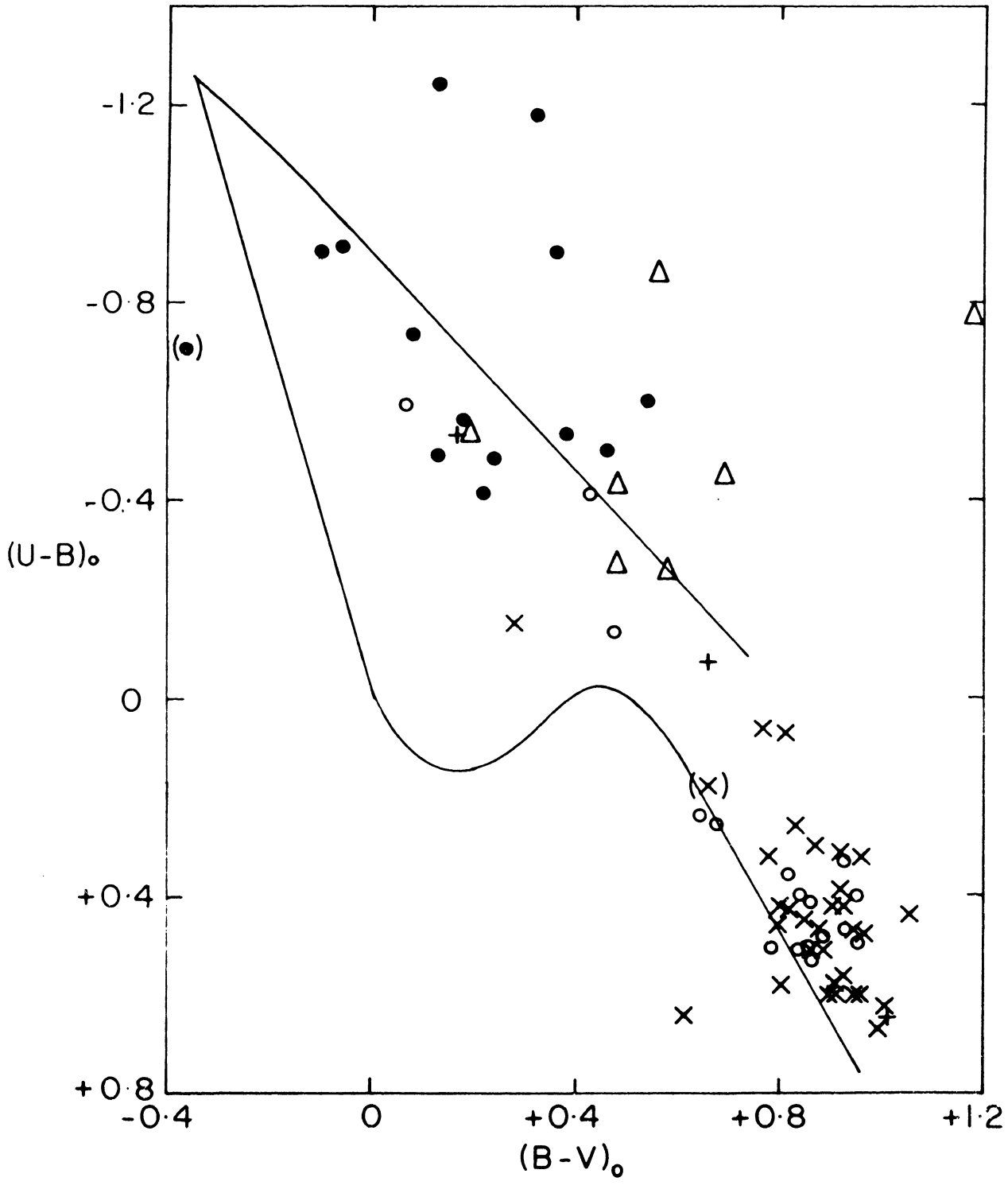

Fig. 4 The two-color diagram. QSO:s are plotted as dots, N galaxies as triangles, other radio galaxies as x, and radioquiet galaxies as open circles. The three plus signs identify in order of increasing $(U-B)_o$ the nuclei of NGC 5236, NGC 1068, and NGC 1316.

(or most of it) and since we are looking for possible correlations between optical and radio data.

We note in Fig. 4 that (1) the separation between the QSO's and the N galaxies is not as complete as in Sandage's two-color diagram (1967a); (2) three bright radioquiet galaxies fall in the QSO-N part of the diagram; (3) the nucleus of NGC 5236 falls likewise among the QSO's; and (4) there is no separation between the radio galaxies and the radioquiet galaxies of type E (D, etc.).

The radioquiet galaxies referred to in (2) are: IC 4662, NGC 7232, and NGC 3955. They, as well as NGC 5236, have emission line spectra with the bluest, IC 4662, showing the highest excitation. IC 4662 has no central condensation, NGC 5236 and NGC 7232 have starlike nuclei, and NGC 3955 has three starlike condensations in its central parts.

The only Seyfert galaxy included in the investigation is NGC 1068. Its nucleus, as measured with an aperture of 7 seconds of arc, occupies in Fig. 4 a position intermediate between the N galaxies and the E galaxies. This indicates amazingly red colors and we will discuss later the possibility of reddening inside the galaxy itself.

The similarity in integrated colors between the radio galaxies and the radioquiet galaxies of morphological type E is further shown in Table 5 in which the observed colors are given for 8 radiogalaxies and for neighboring galaxies of similar morphological type. The only noticable difference occurs for the Virgo galaxies (NGC 4374; 4486). The radio galaxy NGC 4486 is one of the most luminous in the cluster and its redder color may be indicative of giant systems (Cf. de Vaucouleurs 1961). In NGC 4374 Sandage (Wade 1960) has noted dark

lanes which may contribute slightly to its colors.

V. THE RADIO - LUMINOSITY— RADIO INDEX DIAGRAM

Several attempts have been made to establish a diagram for galaxies as useful for interpretations of their evolution as the Hertzsprung - Russell diagram for stars. Heeschen (1960) plotted the absolute radio magnitude at 68.2 cm, $M_{68.2}$, versus a radio color, $m_{21.4}-m_{68.2}$, and derived a clear separation between peculiar and normal galaxies. By "peculiar" Heeschen referred to the strong radio emitters which also showed peculiarities in their optical appearances and/or in their optical spectra. A similar diagram was derived by Pskovskii (1962). Later on Heeschen (1966) discussed the relation between the absolute radio luminosity, L, and the surface brightness, B, both at 1400 Mc/s. Similar diagrams have been discussed by Shklovsky (1962) and by Aizu et al (1964) but with B replaced by the radius and by the volume emissivity, L/V, respectively. The main conclusion is that two distinct sequences exist in the log L, log B diagram. The more luminous one contains the radio galaxies and the QSO:s, the other one contains the spirals and the irregular galaxies. Heeschen suggests that the two sequences represent evolutionary tracks or loci of evolutionary tracks and that the galaxies evolve from small-diameter, high surface brightness objects to large, stable objects with lower luminosity and surface

brightness objects to large, stable objects with lower luminosity and surface brightness.

It is worth recalling in this connection that absolute luminosity, surface brightness relations for normal galaxies have been studied in the photographic region (Holmberg 1958). As it is likely that some important information may escape detection in investigations limited to one frequency or a narrow wavelength region, we would prefer to use a bolometric magnitude or a measure of the intrinsic luminosity at a specified frequency, and a gradient valid for the whole spectrum— provided a unique one really exists. However, at present the intensity distribution over the whole range from low radio frequencies to the optical region is known for only a few objects, and in hardly any case does a unique gradient apply to the whole spectrum. In particular should be mentioned the strong infrared radiation observed in several objects. However, for the definition of a gradient this component may possibly be disregarded if it is due to reradiation of the ultraviolet emission by dust in the objects (cf. Pacholczyk and Weymann 1968).

In order to find comparable data for as many objects as possible we have decided to use the radio index introduced by Brown and Hazard (1961), viz. $(m_r - m_{pg})$, where m_r is the radio magnitude at 158 Mc/s. Brown and Hazard studied the relation between this index and the apparent photographic magnitude for spiral galaxies, correcting for tilt and internal absorption.

In Fig. 5 we have plotted the absolute radio magnitude, M_{158}, versus the radio index $(m_{158} - B)_o$. In order to extend the range

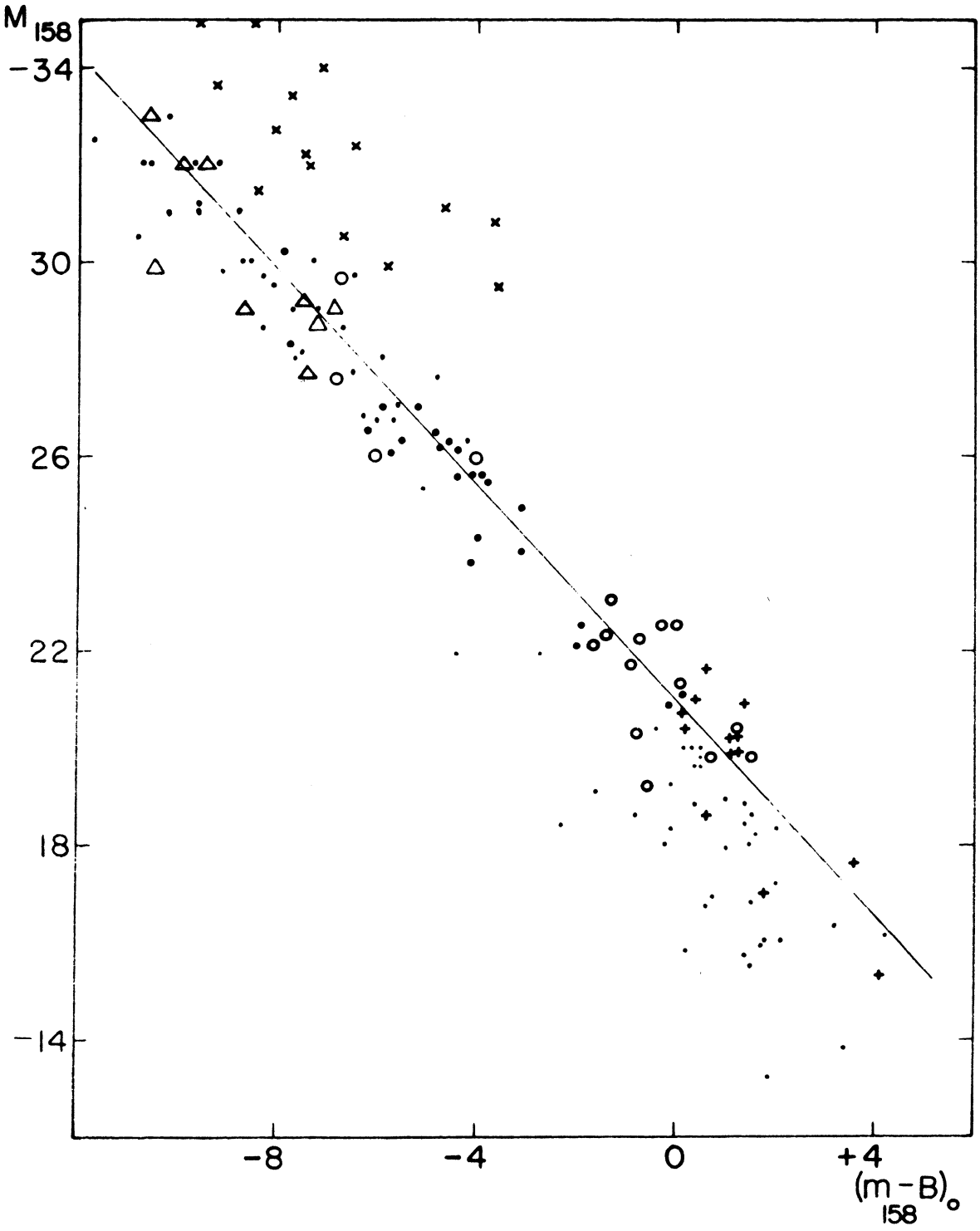

Fig. 5 The absolute radio magnitude - radio index diagram. QSO:s are plotted as x. N galaxies as triangles, radio galaxies in our investigation as dots, Tovmassian's barred galaxies as open circles and his peculiar galaxies as + . Small dots represent radio galaxies from Aizu et al's catalogue. The four large circles mark Arp's objects listed in Table VII. Five objects fall outside the diagram. Two are QSO:s listed in Table VI; the others are 3C 405 (-11:,-37); 3C 348 (-13,-34), and 3C 295 (-14,-36).

in M_{158} we have included data from Aizu et al's catalogue (1964). For the same reason we have also added the objects for which Searle and Bolton (1968) have recently determined the redshifts, as well as the galaxies with known distances in Tovmassian's investigations of peculiar and barred galaxies (1966b,c). All data have been reduced to the present system, i.e. differences in the assumptions about galactic absorption have been taken into account, and a Hubble constant of 100 km/sec/Mpc has been used. (It should be noted that for NGC 1313 we have taken m-M = 28.55 (de Vaucouleurs 1963) instead of Tovmassian's value, m-M = 24.) The data for the most important additional objects are gathered in Table VI.

We note in Fig. 5 that all the "normal" radio emitters, from 3C 295 through the N galaxies to the weak radio galaxies, follow a unique linear relation between M_{158} and $(m_{158} - B)_o$ extending over 20 mag in M_{158}. This relation holds also for the Seyfert galaxies, NGC 1275, NGC 4151, NGC 1068, and 3C120. In the low-luminosity end of the diagram, some galaxies (mostly irregulars) fall well below the straight-line relation. With regard to these weak radio emitters and to the radio-quiet galaxies we refer to Heeschen and Wade (1964) who concluded that most likely all spirals and Magellanic-type irregulars are radio sources. The cases where no radio emission is detected can be understood in terms of the sensitivity limit for detection. A more recent discussion of this problem has been presented by de Jong (1967).

It should be stressed that the photographic magnitudes used are in all cases the integrated magnitudes over the observed portion of the galaxies (which for the largest ones may mean that the magnitudes are at the most 0.5 mag too faint). Similarly, for radio sources with several components, the total radio brightness is used. If for core sources the optical magnitudes of the cores only are used, the corresponding points will be shifted on the average three magnitudes to the left of the present line. We conclude that the straight-line relation depends upon the use of the total energy output of the galaxy at the selected optical and radio frequencies.

The slope of the straight line ($\sim 45^{o}$) shows that virtually all radio galaxies have an absolute photographic magnitude of $M_B = -21$. Only the weakest radio emitters have a significantly lower optical luminosity.

In Fig. 5 are also plotted 15 QSO:s. (Two additional QSO:s are listed in Table VI). The majority falls 4 magnitudes above the linear relation for the normal radio sources, provided their redshifts are considered of cosmological origin. Thus, the QSO:s have an extreme excess in brightness in the optical region as compared with radio galaxies of the same radio brightness. Within the radio frequencies, there is little difference between the QSO:s and the radio galaxies (Burbidge 1967b, p. 420), but the QSO:s have generally flatter radio spectra and show more often high frequency enhancement and/or synchrotron self absorption.

The near-constancy of the absolute photographic magnitude, M_B, for most of the strong radio galaxies, is also seen in the small scatter around the straight-line relation in Sandage's (1967a,b) Hubble diagram for E and N galaxies. Correspondingly, deviations of the Seyfert nuclei to the right and of the QSO:s to the left of the line in Arp's (1968a) Hubble diagram express the facts noted here;

1) that the core sources will follow the same relation as the other radio galaxies only if the total brightnesses at the selected frequencies are used; and 2) that the QSO:s show an appreciable excess radiation in the optical region.

This excess of the QSO:s has to be explained. Strong emission line objects occur outside the QSO group, and these galaxies follow the linear relation well with the possible exception of 3C405 where, however, the galactic extinction plays a decisive role. It appears impossible that the neglected K-correction can have an effect of this order, and any turn-over effect in the radio spectrum, apart from generally occurring at lower frequencies, would affect the radio index as well as the radio luminosity. Similarly, any effect of an infrared component, if it extended to 158 Mc/s, would be included in M_{158} as well as in m_{158}.

We are thus left to consider the radiation in the photographic spectral region. Significant contributions may be expected from a non-thermal and a thermal component. In the QSO:s the non-thermal component dominates; the stellar one is generally considered as

non-existing. In ordinary radio galaxies the stellar component is by far the strongest, whereas it is argued that in some Seyfert galaxies the non-thermal component may be quite strong. Their nuclei fall, however, on the opposite side of the straight line relation in Fig. 5 to the QSO:s. However, if we accept the infrared components as due to an appreciable amount of dust, we should correct the blue magnitudes for the corresponding absorption. In the nucleus of NGC 1068 this may amount to 2 - 3 magnitudes (see below). This would move the nucleus of NGC 1068 almost to the straight line, or the total galaxy less than one magnitude to the right of the line in Fig. 5. If we assume that all objects with strong infrared components should have similar corrections applied to the observed data, we may find that a number of objects are shifted slightly to the QSO-side of the line. It is doubtful, however, that any significant changes of the diagram will occur.

The possibility that the blue excess radiation of the QSO:s is caused by a strong stellar component should also be considered. The integrated spectrum of a series of supernovae may fit the observations. At present this appears perhaps less likely.

Finally, we may discuss the case that the redshifts of the QSO:s are not completely of cosmological origin. If we accept Arp's (1966a) suggestion that 3C 273 is at the distance of the Virgo cluster, it will fall about 2 mag below the straight line in Fig. 5. Similarly, 3C 286, which may be at the distance of the three early-type galaxies NGC 5223, 5228, 5233 (average m_{pg} = 14.5; possible M_{pg} = -19), will fall about

4 mag below the straight line. The possible similarity between the QSO:s and the nuclei of Seyfert galaxies is regained by this shift of the QSO:s, as we have already noted (p.11) that these nuclei fall well to the left of the straight line in Fig. 5 (cf. Fig. 1 in Heeschen 1966) where the QSO:s will drop to the core sources if they are nearby objects. We note that if the "pure" non-thermal emitters fall between two and four magnitudes to the left of the normal radio galaxies in the diagram (Fig. 5), it means that the total radiation in B in the radio galaxies is about 6 to 40 times the non-thermal.

We have remarked above (p.11) that for the multiple radio sources the radiation from all components have been used in plotting the color-magnitude diagram in Fig. 5. Connected with the approach is Arp's (1967, 1968b) suggestions that radio sources form pairs around peculiar galaxies and that radio galaxies are origins for lines of galaxies. We have looked in detail on four of Arp's (1967) objects and computed the total radiation at 158 Mc/s and in B for each of them. The distance of the central galaxy has been adopted for each group. The results are given in Table VII, and the objects are identified by large circles in Fig. 5. Obviously, they all fit the normal radio galaxy relation well. Consequently, there is no contradiction in the present quantities to the idea put forward by Arp. On the other hand no explanation of the large redshifts of the involved QSO:s is given, either.

VI. SURFACE BRIGHTNESS DISTRIBUTIONS AND COLOR DISTRIBUTIONS

So far we have used our multi-aperture observations only as integrated data for a given "maximum" diameter. However, more useful information about the composition of the galaxies is certainly obtained by studying the surface brightnesses and the colors of the various zones contained in the observations. Tifft (1968a,b) has derived some interesting results regarding the true color distribution in the inner regions of galaxies by reducing his multi-aperture colors into true colors for a series of rings. Naturally, caution has to be taken in the interpretation of surface brightnesses derived in this way, as for instance different degrees of ellipticity of the brightness isophotes of a galaxy will tend to smooth the data. However, we have already seen (p.6) that our surface brightnesses agree well with those obtained by microphotometer analysis of the intensity distributions along selected diameters.

Table VII gives for 10 galaxies the surface brightness, S_V, in magnitudes per square second of arc, and the corresponding colors, (B - V) and (U - B) of the zones at the distances, r", from their centers. We define $r^2 = \frac{1}{8}(d_1^2 + d_2^2)$, where d_1 and d_2 are the diameters defining the ring in question. For each galaxy is also given the galactic absorption, A_B, and the distance, D, expressed in the distance of the Virgo cluster as a unit (redshift = 1200 km/sec). In the discussion below, the surface magnitudes and the colors are corrected for galactic absorption, and the angular dimensions of the galaxies are reduced to the distance of the Virgo cluster.

a. The brightness distributions in ultraviolet light and the (U - V) color distributions. - The ultraviolet brightness distributions in the E and SO galaxies, NGC 4374, NGC 4486, IC 4296, and NGC 1316 are compared in Fig. 6. Their U-V colors are plotted in Fig. 7. It is immediately obvious that the four galaxies have very similar brightness distributions outside $r \gtrsim 20''$ (about 10 kpc). Due to its greater distance, IC 4296 has not been resolved inside this radius. Preliminary analysis of plates of this galaxy indicate, however, that the brightness distribution in its core region is similar to that of NGC 4374. The similarity between these two galaxies is also obvious in the U-V color distributions.

NGC 4486 has a higher surface brightness than NGC 4374 except in the core itself (i.e. inside r = 5" or about 2.5 kpc). The latter galaxy has a semistellar nucleus whereas NGC 4486 lacks a sharp nucleus. This was also noted by Spinrad (1962). In his classification system, the nucleus of NGC 4486 shows D: (dwarf) characteristics, whereas that of NGC 4374 shows G (giant) characteristics. He suggests that a possible explanation of the fact that type D systems are more luminous and massive may be that they contain great numbers of intrinsically faint stars. However, NGC 4486 is obviously not significantly more luminous than NGC 4374 in any part of the range covered by our observations. Its total brightness is about 0.6 mag brighter than that of NGC 4374; this "excess" has obviously to come from the outer parts with a probably insignificant contribution from the jets. We recall in this connection that

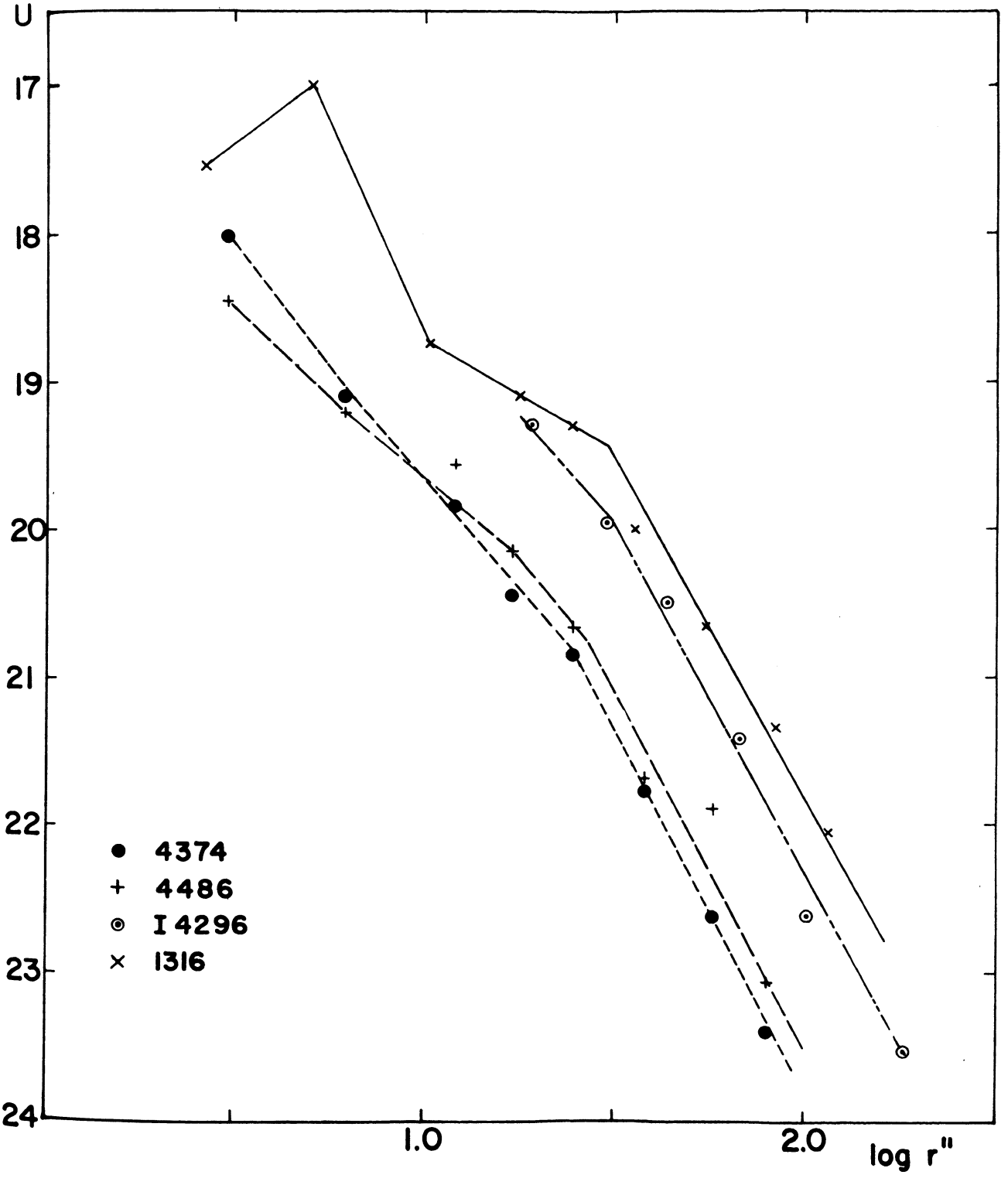

Fig. 6 The brightness distributions in ultraviolet light (unit in U is mag/□") for some early-type galaxies. The linear scale is for the distance of the Virgo cluster.

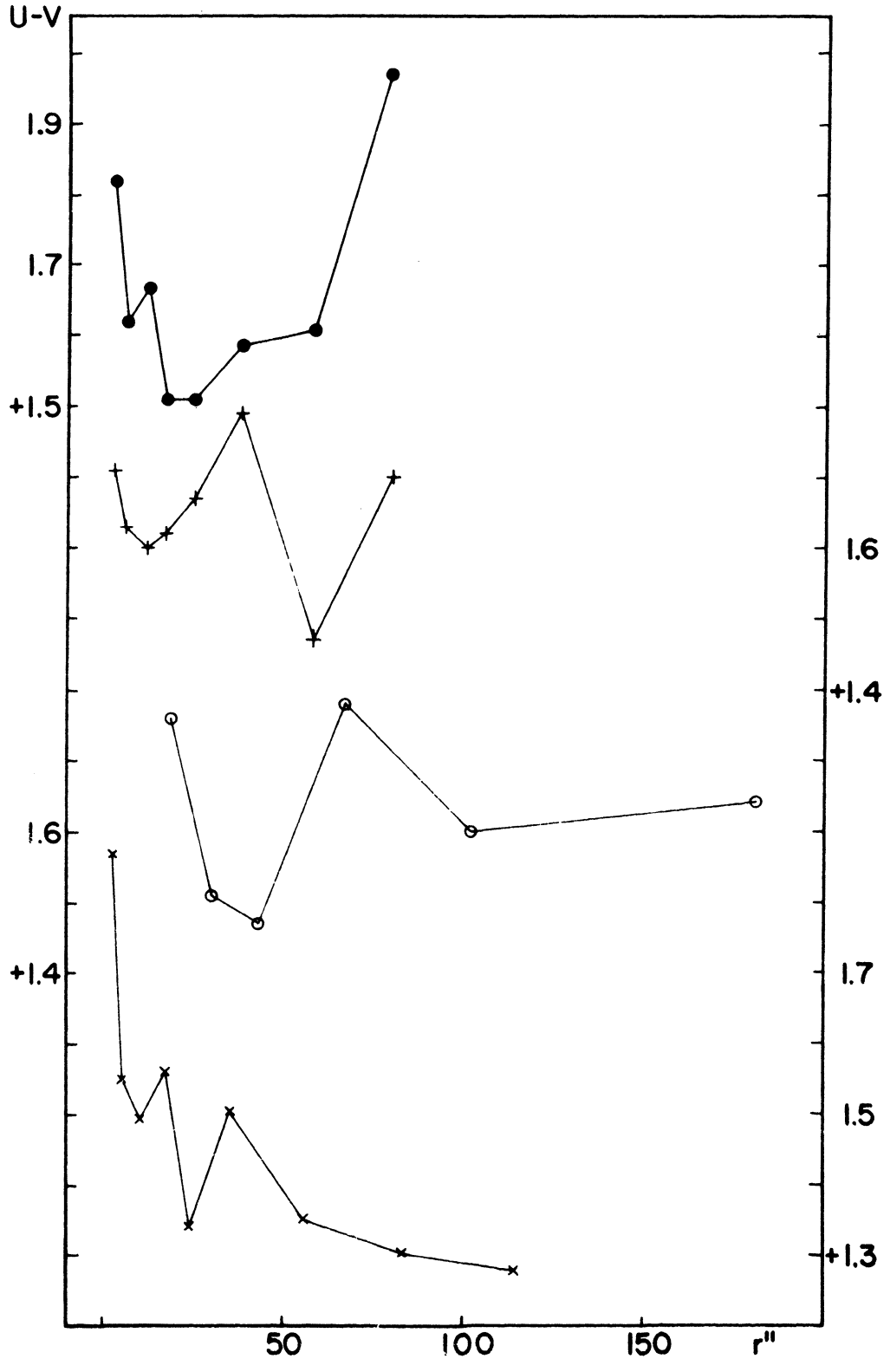

Fig. 7 The U-V distribution for the galaxies in Fig. 6.

Sandage has observed some weak absorption lanes in the centre of NGC 4374 (Wade 1960), and we repeat also the well known fact that NGC 4486 has a huge number of globular clusters.

A further similarity between the three elliptical galaxies is that the colors decrease from the fairly red nuclei into a less red zone upon which they apparently increase in another red zone. The conditions in NGC 4486 are appreciably more confused than in the two others. Further discussion of the color variations will be given below (p.20). Here we will compare our results with those derived by Markaryan et al (1965). In spite of the fact that 1) our values are smoothed over all directions whereas theirs are obtained along selected radii, and 2) that the color indices used are (U - V) and (m_{pg} - m_v), respectively, the similarities are striking. Our results for NGC 4374 and NGC 4486 confirm that 1) the color in elliptical and lenticular galaxies change rather appreciably, and 2) there is a sharp decrease in the color indices in the immediate vicinity of the nuclei, after which they increase (to a distance equal to approximately one third of the radius of the galaxy), and then begin to decrease intensively. Tifft's (1968a,b) color curves for the E galaxies in the Virgo cluster do not show the nuclear reddening of the Ep class (to which NGC 4486 belongs), nor do they reach sufficiently far out to show the outer red zone clearly.

The most luminous of the 4 galaxies in this group, NGC 1316, has in the core region a more extreme increase in color as well as a pronounced decrease in ultraviolet surface brightness. It has

been suggested (Sersic 1957) that the contribution of the dust lanes to the color of the nucleus of NGC 1316 is insignificant. However, the most reasonable explanation of the decrease in brightness in the core proper (this decrease occurs in all colors) is the assume an interior absorption. A color excess of about $E_{B-V} = 0.15$ mag for the core itself is obtained by comparing it with the colors of the innermost rings. This corresponds to an absorption of about 0.5 mag in V and 0.7 mag in U. The application of these corrections will bring the "true" brightness distribution of NGC 1316 into fair agreement with those of the other galaxies in Fig. 6.

Fig. 8 shows the brightness distributions in ultraviolet light and the U - V variations for NGC 1068, NGC 5236, and NGC 6872 with the corresponding data for NGC 4374 repeated for comparison. The difference in U between NGC 1068 and NGC 4374 may appear great but is in fair agreement with their integrated absolute magnitudes. The brightness distributions of these two galaxies are otherwise, surprisingly similar (see below). We note that NGC 5236 has an extreme increase in intensity in U in the core and a very red zone immediately outside it. NGC 6872 has a pronounced nucleus and extensive spiral arms. It is not surprising to find that its inner regions are similar to an E galaxy's.

The similarity in shape between the color curves for NGC 1068 and NGC 5236 are striking. Though the extremes are reached by NGC 5236 only, it appears obvious to search for an explanation of the color distribution applicable to both galaxies. This will, however,

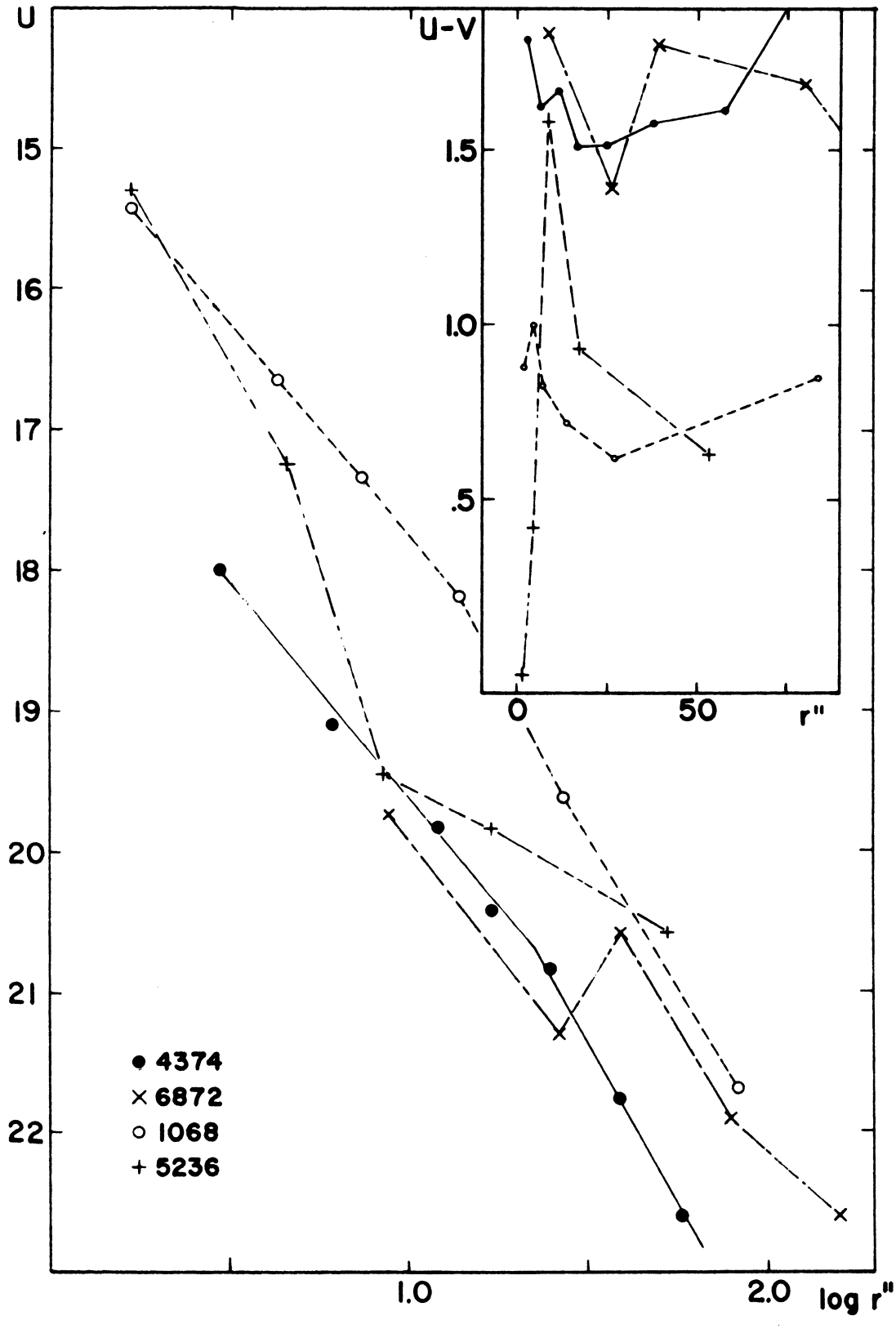

Fig. 8 The brightness distributions in ultraviolet light (scales as in Fig. 6) for three spiral galaxies. NGC 4374 is given for comparison. The insert gives the corresponding U - V distributions.

be more obvious in the discussion of the two-color diagram, below.

b. The two-color diagrams. In section IV we discussed the two-color diagram for all our objects, using the integrated colors (corrected for galactic absorption). Here, we will discuss two-color diagrams of the larger galaxies, plotting the individual values for the various zones (all corrected for galactic absorption). It should be noticed that by using the values in Table 7 we plot colors for points that are not at the same linear distances from the cores of the galaxies. This is of little importance except as far as the interpretation of the "core" colors themselves are concerned. The so called "nucleus" in IC 4296 includes for instance a portion of the galaxy which extends to 20" at the distance of the Virgo cluster. Similarly, the "nucleus" of NGC 1947 has a 12" radius at that distance, NGC 6876 has a 10" radius, and so on. Generally, effects of this type as well as the possibly abrupt composition variations near the nuclei of galaxies have been neglected, and results have been presented as representative for the cores when they in reality refer to a fairly large portion of the galaxy. Note for instance that the red nuclei of the elliptical galaxies in the Virgo cluster have radii smaller than about 3 seconds of arc. A circular aperture of 17" (Wood 1966) includes already a large amount outside the semistellar nucleus. If we take the values for NGC 4374, we find that its magnitude inside an 8" diaphragm is 12.31. The zone added to this in the smallest aperture used by Wood has the same apparent magnitude as the nucleus itself, and

the one added by McClure and V. D. Bergh is 1.3 mag brighter (in B) than the nucleus itself. Moreover, the colors of the added zone are (0.90; 0.58) as compared with those of the nucleus (1.04; 0.65) or in other words, the zone acts as a K2V star whereas the nucleus is more like a "Baade giant or subgiant". Similar conclusions may be drawn for Spinrad's observations (1962), whereas his recent studies of M 31 are carried out with a much smaller aperture (9 seconds of arc, 1968).

It is not our intention to synthesize models to fit our U,B,V colors as there are too many possible combinations. We will, however, read the diagrams as directly as possible, bearing in mind the information already available from previous observations of these or similar galaxies.

The two-color diagrams showing the color variations in the larger galaxies are presented in Figs. 9 and 10. The standard main sequence relation is drawn in all figures, and in Fig. 9b we have also marked the relation for the giant and subgiant branch in M3 (Sandage and Eggen 1959). The innermost region observed is marked as a dot in a circle in the diagrams, and the observed points for each galaxy are connected by straight lines to simplify the reading of the diagrams.

The E and SO galaxies. Although their nuclei are generally slightly off the main sequence relation, a large portion of these galaxies have colors matching the main sequence stars very well. It is unfortunate that in the U,B,V system the luminosity class III

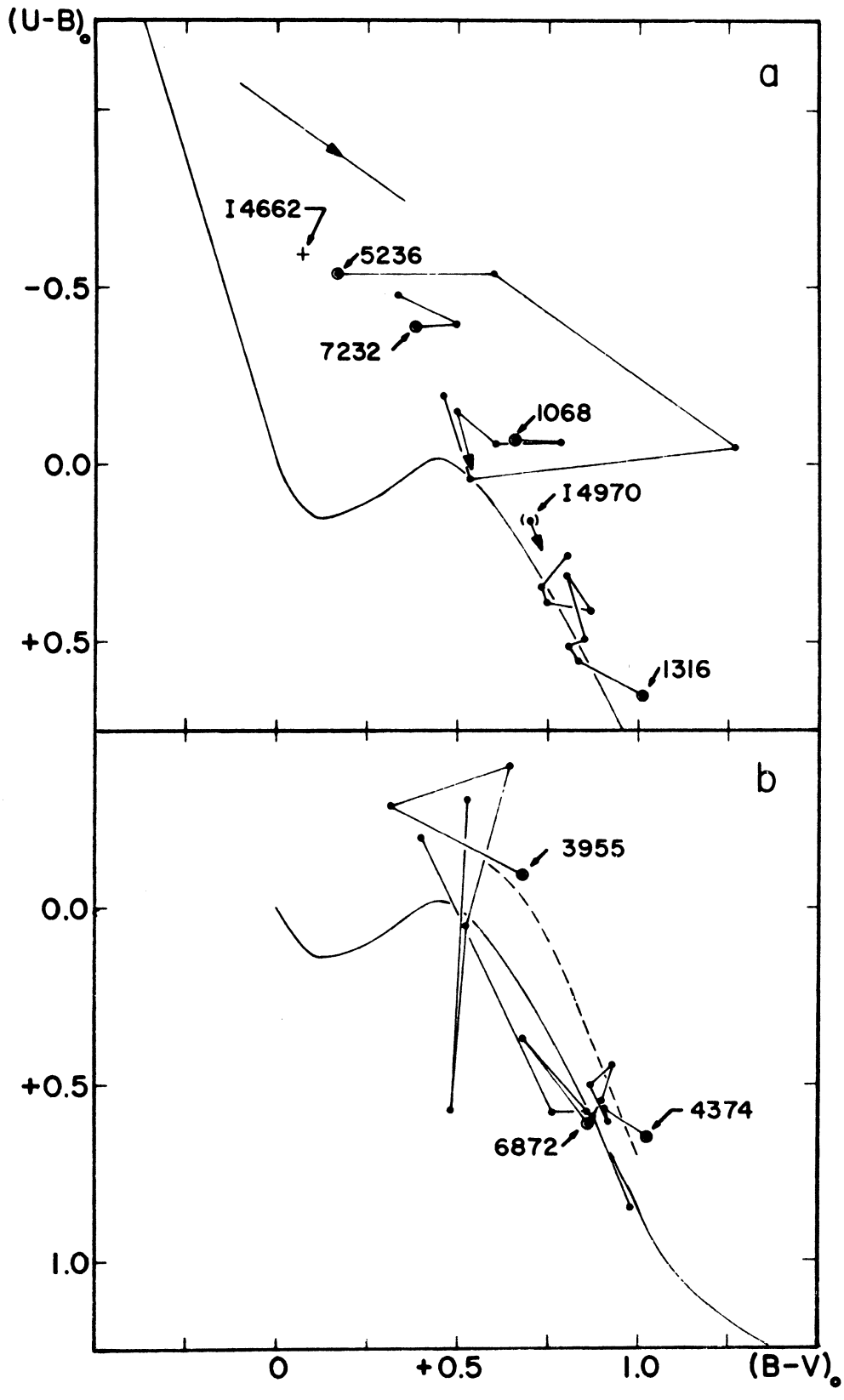

Fig. 9 The two-color diagram for some of the larger galaxies. The core regions (defined in Table 8) are plotted as dots in circles. The standard relation for the main sequence is drawn, and, in addition, in Fig. 9b the relation for the giant and sub-giant branch in M3.

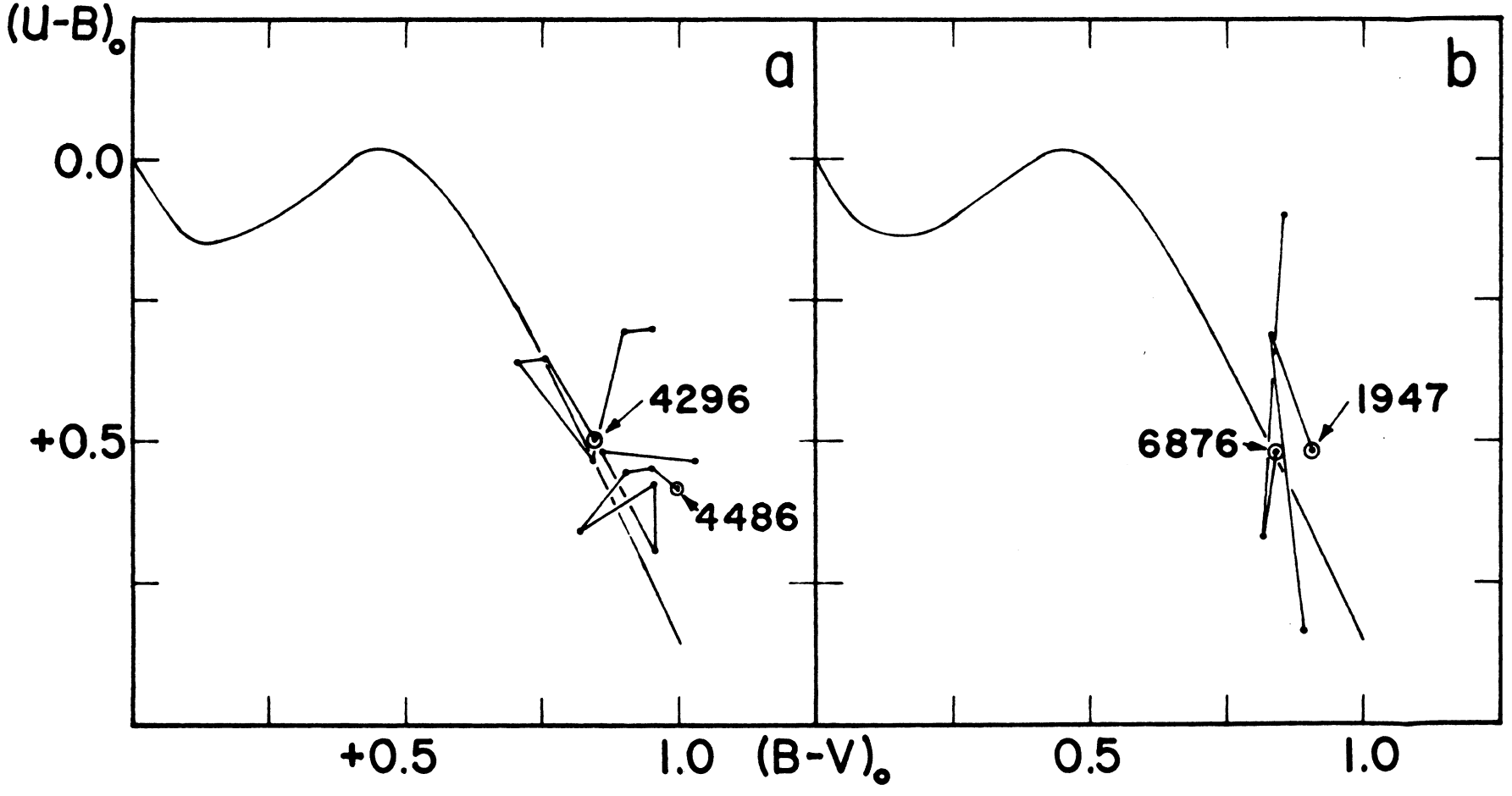

Fig. 10 The two-color diagram for some of the larger galaxies (Cf. Fig. 9).

relation approaches the class V relation closely from about B-V = 0.75 on, so that no separation into giants and dwarfs can be obtained.

The outer portions of NGC 4486, IC 4296, and NGC 6876 appear to have an ultraviolet excess of the type that may be explained by metal poor halosystems. NGC 4374 and NGC 1947 reach in the outer portions fairly red "main-sequence" type colors. In the case of the latter galaxy it must be noted that possibly the fairly rich stellar background, due to the Large Magellanic Cloud, may contribute.

IC 4970 has fairly blue colors for an SO galaxy and may be a dwarf system (cf. de Vaucouleurs 1961). The innermost point plotted represents the second zone in Table VII, as the central zone is disturbed by a star. We have already pointed out that the nucleus of NGC 1316 is affected by dark lanes. Corrections for the suggested color excesses will move the core values onto the main sequence relation. Its outer portions are slightly blue, but in this case it is probably more reasonable to assume that a number of early-type stars may exist in the possible spiral structure.

The spiral and the irregular galaxies. We have plotted the values for IC 4662, the bluest of the emission-line galaxies, as a reference point. If we consider that the position of this galaxy in the two-color diagram, slightly off the O,B star relation, is typical for a predominantly blue population with only some additional red stars, we may explain the increasing colors of the nuclei of NGC 5236, 7232,

and 1068 as showing as increasing contribution of the older population. However, this is contradicted by the fact that NGC 1068 has the most active nucleus. Therefore, it appears more reasonable to explain the increasing colors as due to absorption in the galaxy itself.

Our observations of NGC 5236, NGC 7232, and NGC 1068 include almost the same portions of the galaxies with the smallest aperture used. If we accept the same population mixture in all of them and consider the contribution of the emission lines to the colors to be the same, we can readily understand why the three nuclei are displaced more or less along the reddening line. (We may, of course, go one step further and follow all three galaxies back to the main sequence relation, assuming that the later types do not contribute significantly to these colors).

In favor of the latter explanation are also the observations that the nuclei of these spirals are not as outstanding in the observed surface brightness-log r diagrams as might be expected. Furthermore, in the case of the NGC 1068 the intensity distribution in U appears too similar to that of an E galaxy. Therefore; it seems reasonable to accept a certain amount of reddening by dust in the galaxy itself. The nucleus of NGC 1068 has a color excess of about E_{B-V} =0.5 mag as compared with IC 4662 and of E_{B-V} =0.8 mag if followed along the reddening line to the main sequence relation.

A most noticable effect occurs in NGC 5236 where an extreme reddening in B-V occurs immediately outside the nucleus. This is not

easily explained as a tremendous increase in the number of red stars, as this would have increased the U-B color more than measured here, nor it it explained by a sudden disappearance of all emission lines when we leave the nucleus. We suggest that it is due to interstellar reddening and that the nucleus of NGC 5236 suffers heavily from absorption out to a distance of 20 seconds of arc. Outside this region, in the spiral-arm zones, we find a typical mixture of disk and arm population (cf. NGC 3031 and NGC 4736, Simkin 1967).

In his two-color diagram for irregulars de Vaucouleurs (1961) noticed a large scatter. One of the main reasons for this is probably that integrated colors were used. It is easy to see that practically any color combination can be derived for NGC 3955. (See p. 28). In addition a varying amount of absorption as well as of population mixture would scatter the galaxies to the extent noted in his diagram.

VII. CONCLUSIONS

We have found (Fig. 5) that most of the radio galaxies have a constant absolute photographic magnitude in spite of a tremendous range in radio luminosity. We interpret this as due to a strong stellar population dominating the radiation in the blue spectral region for an appreciable part of the active time of the radio galaxies. The optical synchrotron radiation supposedly existing in many core sources (in particular in Seyfert galaxies) may be isolated

by observations of the nuclei, though it is not yet quite clear to what extent absorption by dust in the core regions leads to a misinterpretation of the observations.

The QSO:s, at cosmological distances, fall well away from the normal radiogalaxy relation in Fig. 5, and they differ in this respect from the N galaxies as well as from the Seyfert galaxies. If we accept the strong optical synchrotron radiation in the QSO:s as an indication of extreme youth of the whole object, our diagram may be read in terms of evolution of galaxies in the following way: They evolve from small-diameter objects with high radio and optical luminosity (both due to synchrotron radiation), first by a weakening of the optical synchrotron radiation until a strong stellar component (is formed and) dominates. From then on the optical luminosity of the whole object remains practically constant, whereas the radio luminosity decreases fairly continuously. Flares in the nuclei may occur and are seen in Seyfert galaxies. (We may consider QSO:s and Seyfert nuclei related in the way as Wolf-Rayet stars and planetary nuclei are related.) N galaxies represent then a transit stage between the most luminous QSO:s and the normal radio galaxies. Towards the end of the active period of a radio galaxy the optical luminosity starts to decrease. The point where this occurs is, naturally, not well defined. To this may contribute that optically luminous but radioquiet galaxies may be connected with radio sources in the way suggested by Arp (1967, 1968b). In such cases a whole group of

galaxies and radio sources may have to be considered as one unit.*

The evolution pictured here does not necessarily mean that all galaxies start their "stellar" life at the very maximum of the radio luminosity, nor does it imply that E galaxies evolve into spirals or irregulars. The dominating optical feature in the radio galaxies is the nucleus, and weak spiral structures around bright nuclei in distant objects could easily escape detection. (The diameter of the N galaxy or compact galaxy, Parkes 05 21 - 36, is about 4 kpc (Westerlund and Stokes 1966); at the corresponding distance from the center the surface brightness in NGC 5236 has dropped 4 magnitudes.)

Many of the weak radioemitters are irregular galaxies of Magellanic Cloud type. The combination of an extremely young Population I with an old Population II and synchrotron radio radiation from an extended source (no nucleus) makes it probable that they have been formed as components of older systems; for this assumption speaks also the fact that practically all of them are members of groups of galaxies.

---

* If the QSO:s are nearby objects they are probably connected with galaxies in the way suggested by Arp (1967) and their evolution would have to be considered either in connection with the just-discussed groups or with the components in the multiple radiosources. In the latter case the step from a "pure" synchrotron radio source to an optically visible source may be difficult to visualize.

In Sections II and VI we have shown that multi-aperture photoelectric photometry can be used efficiently for studying the variation of the surface brightness in many types of galaxies, as long as the imposed smoothing is kept in mind. The brightness distribution in ultraviolet light has been found extremely useful, in particular when combined with the change in colors as shown in the two-color diagrams (Fig. 9 and 10). It appears important to study galaxies like NGC 4374 and NGC 4486, which have the same morphological type but a different color variation in the outer portions, using high scale photographs for isodensitometry in several colors. Likewise, the absorption suggested by us to exist in the central regions of several galaxies should be investigated by careful mapping of those regions in several colors.

APPENDIX. COMMENTS ON INDIVIDUAL GALAXIES

NGC 4486 is a well-known core-halo type radio source. The core cource is double and the two components may be connected with the optical jet and the counterjet (Moffet 1968). The most recent discussions of the optical jet have been presented by Felten (1968) and de Vaucouleurs et al (1968). For the 7".5-15" zone we have determined the contribution of the jet to be V = 13.4; B-V=+0.6; U-B=+0.05. As the values have to be derived from estimates of the contribution of the galaxy to the observed total surface brightness at r = 12", the uncertainties are fairly great.

NGC 4486 is among the strong radio emitters and peculiar galaxies discussed by Arp (1967, 1968b). He remarks that the line which may be drawn through the two jets points almost exactly to NGC 4374. He considers NGC 4374 as a case of secondary, cascading ejection or fragmentation, the galaxy itself being once ejected from NGC 4486. Our observations do not permit any decisive conclusions. We call attention to the possible differences between the two galaxies (in addition to the jets) 1) the nuclei are different; 2) there are possibly dust lanes in NGC 4374; and 3) the outer regions have quite different color distributions. To this should be added that Spinrad (1962) finds that NGC 4374 has G and NGC 4486 D: characteristics.

IC 4296 is also one of the strong radio emitters discussed by Arp (1967, 1968b). Gardner and Davies (1964) have suggested that the radio data indicate that there may have been more than one explosion in IC 4296 and that the outer lobes represent the first explosion after the expansion, separation from the parent galaxy and lowering of the radio surface brightness. There are, according to Arp, no conspicuous alignments of smaller galaxies in the vicinity of IC 4296. The explosions in this galaxy are then probably relatively recent events. Arp also suggests that IC 4296 may have been ejected from NGC 5128. This necessitates placing it at the distance of the latter in spite of the fact that its redshift suggests a distance about three times larger. This redshift gives the galaxy an absolute magnitude which fits the straight-line relation in Fig. 5 well.

Acceptance of the shorter distance leads to an absolute photographic magnitude for IC 4296 of only $M_{pg} = -16.4$ mag. This is extremely low for a strong radio source, and it would give IC 4296 a unique position in our diagram (Fig. 5). We are, consequently, inclined to accept the distance for IC 4296 as obtained from the redshift.

We note further that NGC 5128, from the data in Aizu et al's paper (1964), falls on the straight line relation in the $M_{158}/m_{158}-m_{pg}$ diagram. (So does also NGC 5236 in our diagram, and Arp's statement in his Table II (1968b) that this source is too weak for its optical brightness does appear incorrect.) It appears therefore unlikely that NGC 5128 and IC 4296 can belong to the same group.

The spectrum of NGC 1316 has been classified GK by the de Vaucouleurs (1961). In their discussion of the spectrum they express doubts that the galaxy is "the extreme supergiant system that membership in the Fornax cluster would imply". The radio luminosity derived from the redshift (which agrees well with the cluster redshift) satisfies our $M_{158}/(m_{158}-B)_o$ relation, however, so the distance of NGC 1316 appears to be very similar to that of the Fornax cluster.

NGC 3955. This galaxy has been discussed by Tovmassian (1966a) who in a ring-like structure outside the nucleus saw the result of a giant explosion, and by Hodge (1966) who did not detect any pronounced H-alpha emission. The color variations are pronounced in our diagram. The bluest colors are reached in the zone including the three ultraviolet knots in the visible main body of the galaxy. We have already suggested that corrections for reddening will

move the nucleus up in the direction of IC 4662. The effect of the excentrically situated ring,which Tovmassian described,is apparently drowned in other effects.

NGC 6872 and IC 4970 are probably interacting (de Vaucouleurs 1964). It is of interest to note that the colors indicate that the latter may be a low-luminosity lenticular.

REFERENCES

Abell, G. O. 1958, Astroph. J. Suppl. Ser. 3, 211.

Aizu, K., Fujimoto, Y., Hasegawa, H., Kawabata, K. and Taketani, M. 1964, Prog. Theor. Phys. Suppl. 31, 35.

Arp, H. 1966, Science 151, 1214.

Arp, H. 1967, Astroph. J. 148, 321.

Arp, H. 1968a, Astroph. J. 153, L33.

Arp, H. 1968b, Publ. A.S.P. 80, 129.

Bolton, J. G., Clarke, Margaret E. and Ekers, R. D. 1965, Aust. J. Phys. 18, 627.

Bolton, J. G., and Ekers, Jennifer 1966a, Aust. J. Phys. 19, 275.

Bolton, J. G., and Ekers, Jennifer 1966b, Aust. J. Phys. 19, 559.

Bolton, J. G., and Ekers, Jennifer 1966c, Aust. J. Phys. 19, 713.

Bolton, J. G., and Ekers, Jennifer 1967, Aust. J. Phys. 20, 109.

Bolton, J. G., Gardner, F. F., and Mackey, M. B. 1964, Aust. J. Phys. 17, 340.

Bolton, J. G. and Kinman, T. D. 1966, Astroph. J. 145, 951.

Brown, R. Hanbury and Hazard C. 1961, M.N.R.A.S. 122, 479.

Burbidge, E. M. 1967a, Astroph. J. 149, L.51.

Burbidge, E. M. 1967b, Ann. Rev. Astr. and Astroph. 5, 399.

Day, G. A., Shimmins, A. J., Ekers, R. D., and Cole, D. J. 1966, Aust. J. Phys. 19, 35.

De Jong, M. L. 1967, Astroph. J. 150, 1.

Ekers, R. D., 1967 Thesis, Aust. Nat. Univ. Canberra.

Ekers, R. D. and Bolton, J. G. 1965, Aust. J. Phys. 18, 669.

Felten, J. E. 1968, Astrophys. J. 151, 861.

Gardner, F. F. and Davies, R. D. 1964, Nature 201, 144.

Heeschen, D. S. 1960,Publ. A.S.P. 72, 368.

Heeschen, D. S. 1966, Astroph. J. 146, 517.

Heeschen, D. S. and Wade, C. M. 1964, Astron. J. 69, 277.

Hodge, P. W. 1966, Astrophys. J. 146, 593.

Holmberg, E. 1958, Lund Medd. Ser II, No. 136.

Houten, C. J. van 1961, B.A.N. 16, 1.

Howard, W. E. and Maran, S. P. 1964, Astroph. J. Suppl. Ser. 10.

Johnson, H. L. 1954, Astroph. J. 119, 181.

Johnson, H. L. 1955, Ann d'Astroph. 18, 292.

Kinman, T. D., Bolton, J. G., Clarke, R. W. and Sandage, A. 1967, Astroph. J. 147, 848.

Kinman, T. D., and Burbidge, E. M. 1967, Astroph. J. 148, L59.

McClure, R. D. and Bergh, S.v.d. 1968, Astron. J. 73, 313.

Maltby, P., Matthews, Th. A., and Moffet, A. T. 1963, Astroph. J. 137, 153.

Markaryan, B. E., Oganesyan, E. Ya. and Arakelyan, S. N. 1965, Astrofizika-Astrophysics 1, 23.

Moffet, A. T. 1968, Publ. A.S.P. 80, 16.

Pacholczyk, A. G. and Weymann, R. J. 1968, Astron. J. (in press).

Price, R. M. and Milne, D. K. 1965., Aust. J. Phys. 18, 329.

Pskovskii, Yu. P. 1962, Astron. Zhur. 39, 222.

Sandage, A. 1967a, Astroph. J. 150, L9.

Sandage, A. 1967b, Astroph. J. 150, L177.

Sandage, A.R. and Eggen, O. J. 1959, M.N.R.A.S. 119, 278.

Schmidt, M. 1965, Astroph. J. 141, 1.

Searle, L. 1965, Nature 207, 1282.

Searle, L. and Bolton, J. G. 1968, Astroph. J. (preprint).

Sersic, J. L. 1957, Revista Ast. 29, No. 13.

Sersic, J. L. 1961, Z.f. Astroph. 53, 256.

Shane, C. D. and Wirtanen, C. A. 1967, Publ. Lick Obs. 22, Part I.

Shimmins, A. J., Day, G. A., Ekers, R. D. and Cole, D. J. 1966, Aust. J. Phys. 19, 837.

Shklovsky, I. S. 1962, Astr. Zh., 39, 591 (Soviet Astr. - A. J., 6, 465).

Simkin, S. M. 1967, Astron. J. 72, 1032.

Spinrad, H. 1962, Astroph. J. 135, 715.

Spinrad, H. 1968, Publ. A.S.P. 78, 367.

Tifft, W. G. 1968a, Astron. J. (in press).

Tifft, W. G. 1968b, Astron. J. (in press).

Tovmassian, H. M. 1966a, Astrophysica 2, 235.

Tovmassian, H. M. 1966b, Aust. J. Phys. 19, 565.

Tovmassian, H. M. 1966c, Aust. J. Phys. 19, 883.

Vaucouleurs, G. de 1961, Astroph. J. Suppl. Ser. 5, 233.

Vaucouleurs, G. de 1963, Astroph. J. 137, 720.

Vaucouleurs, G. de and Vaucouleurs, A. de 1961, Mem. R.A.S. 68, 11.

Vaucouleurs, G. de and Vaucouleurs, A. de 1964, Reference Catalogue of Bright Galaxies. University of Texas Press.

Vaucouleurs, G., Angione, R. and Fraser, C. W. 1968, Univ. of Texas, McDonald Obs. Preprint No. 5.

Wade, C. M. 1960, The Observatory 80, 235.

Wade, C. M. 1968, Astron. J., (in press).

Walker, M. F. 1968, Astroph. J. 151, 71.

Walker, M. F. and Hayes, Sethanne 1967, Astroph. J. 149, 481.

Westerlund, B. E. 1963, M.N.R.A.S. 127, 71.

Westerlund, B. E. and Smith, Lindsey F. 1966, Aust. J. Phys. 19, 181.

Westerlund, B. E. and Stokes, N. R. 1966, Astroph. J. 145, 354.

Westerlund, B. E. and Stokes, N. R. 1968, unpublished.

Westerlund, B. E. and Wall, J. V. 1968, Astron. J., in press.

Westerlund, B. E. Wall, J. V. and Stokes, N. R. 1967, Proc. Astr. Soc. Aust. 1, 23.

Wills, D. 1967, Astroph. J. 148, L57.

Wood, D. B. 1966, Astroph. J. 145, 36.

Legend to the figures:

Fig. 1 Comparison of multi-aperture observations of NGC 4374 and NGC 4486. Observations by us are plotted as dots, by Tifft as open circles, and by de Vaucouleurs as x.

Fig. 2 Comparison of multi-aperture observations of NGC 1068. Observations by us are plotted as dots, by Sandage as +, and by Chincarini as open circles.

Fig. 3 Comparison of observed surface brightnesses in blue light in NGC 1068 and in NGC 4486. Unit in B is mag/□". Our observations are plotted as dots, van Houten's as open circles, Markaryan et al's as + , and Tifft's as half-filled circles.

Fig. 4 The two-color diagram. QSO:s are plotted as dots, N galaxies as triangles, other radio galaxies as x, and radioquiet galaxies as open circles. The three plus signs identify in order of increasing $(U-B)_o$ the nuclei of NGC 5236, NGC 1068, and NGC 1316.

Fig. 5 The absolute radio magnitude - radio index diagram. QSO:s are plotted as x, N galaxies as triangles, radio galaxies in our investigation as dots, Tovmassian's barred galaxies as open circles and his peculiar galaxies as + . Small dots represent radio galaxies from Aizu et al's catalogue. The four large circles mark Arp's objects listed in Table VII. Five objects fall outside the diagram. Two are QSO:s listed in Table VI; the others are 3C 405 (-11:,-37); 3C 348 (-13,-34),and 3C 295 (-14,-36).

Fig. 6 The brightness distributions in ultraviolet light (unit in U is mag/□ ") for some early-type galaxies. The linear scale is for the distance of the Virgo cluster.

Fig. 7 The U-V distribution for the galaxies in Fig. 6.

Fig. 8 The brightness distributions in ultraviolet light (scales as in Fig. 6) for three spiral galaxies. NGC 4374 is given for comparison. The insert gives the corresponding U - V distributions.

Fig. 9 The two-color diagram for some of the larger galaxies. The core regions (defined in Table 8) are plotted as dots in circles. The standard relation for the main sequence is drawn, and, in addition, in Fig. 9b the relation for the giant and sub-giant branch in M3.

Fig. 10 The two-color diagram for some of the larger galaxies (Cf. Fig. 9).

TABLE I. PHOTOMETRY QSO's.

Parkes Catalogue Number	Finding Chart	J.D. 2439000	V	B-V	U-B
0022-29	(1)	448	17.91	+0.34	-0.40
0119-04	(4)	447	17.03	+0.46	-0.82
0130-17	(3)	449	18.44	+0.46	-0.27
0155-10	(4)	449	17.09	+0.23	-0.41
0202-76	(8)	445	16.77	+0.06	-0.77
0440-00	(4)	445	19.22	+0.37	-1.05
1233-24	(2)	236	17.25	+0.36	-0.42
		269	17.18	+0.36	-0.74
1327-21	(1)	233	16.63	+0.22	-0.62
1420-27	(2)	230	17.70	+0.57	-1.04
		232	17.81	+0.67	-1.19
		369	17.83	+0.55	-0.66
1422-29	(2)	236	16.72	+0.61	-0.17
		269	16.95	+0.43	-0.18
2111-25	(2)	440	19.1	-0.7:	-0.6:
2115-30	(1)	270	16.39	+0.70	-0.47
2135-14	(4)	440	15.81	+0.10	-0.78
2223-05	(3)	441	15.79	+0.60	-0.39

Parkes Catalogue Number	m_r	l_{II}	b_{II}	Remarks
0022-29	7.9	13^o	-84^o	
0119-04	9.9	142	-66	On J.D. 2439410: V=16.88; B-V=+0.46; U-B=0.72 (10). Spectrum and redshift in (11).
0130-17	11.6	168	-76	
0155-10	8.6	169	-67	
0202-76	8.8	297	-40	
0440-00	10.4	197	-28	
1233-24	8.6	299	+38	UV excess less marked photographically (6).
1327-21	9.1	315	+40	V=16.74; B-V=+0.10; U-B=-0.54 (9).
1420-27	8.1	327	+31	
1422-29	8.5	326	+29	
2111-25	10.5	22	-42	V=16.47; B-V=+0.49; U-B=-0.54 (9).
2115-30	8.9	16	-43	Redshift by Searle and Bolton (1968).
2135-14	8.4	38	-44	On J.D. 2439322; V=15.53; B-V=+0.10; U-B=-0.83(10). Spectrum and redshift in (11).
2223-05	8.3	59	-48	3C446. For references see p.582 in IAU Draft Report for 13th General Assembly 1967.

TABLE II. PHOTOMETRY OF N GALAXIES

Parkes Catalogue Number	*Finding Chart*	*J.D. 2439000 +*	V	B-V	U-B	m_r	l_{II}	b_{II}	Remarks
0000-17	(3)	440	16.77	+0.70	-0.16	9.0	71^o	-75^o	Remark on spectrum by Searle and Bolton (1968).
0518-45	(8)	446	15.77	+0.87	-0.31	5.2	251	-35	Pictor A. Spectrum and redshift in (13). Interforometry at 470 and 1400 MHZ indicates the probability of 4 components: one pair 3'x1'.5 in size separated by 4'.1 in P.A. 105^o, and another pair $<$ 0'.5 in size, separated by 6'.9 also along P.A. 105^o (8).
0521-36	(1)	152	14.48	+0.68	-0.28	7.3	240	-33	Spectrum and redshift in (15). At 86 MHZ d=20'; at 960 MHZ d $<$ 1'.0. See also Searle and Bolton (1968).
		153	14.45	+0.65	-0.30				
0533-12	(3)	232	17.09	+1.45	-0.54	9.1	2.5	-22	
		233	16.98	+1.54	-0.84				
0634-20	(1)	233	17.58	+0.69	-0.19	7.5	230	-12	Classified E in (1). Radio structure discussed in (8): At 2700MHZ two components of equal intensity but asymmetric and separated by 11' along P.A.=0^o. Redshift by Searle and Bolton (1968).
1417-19	(3)	230	16.57	+0.65	-0.90	9.1	330	+39	Spectrum and redshift in (7).
		232	16.42	+0.92	-0.65				
		269	16.65	+0.71	-0.56				
1514-24	(1)	233	15.16	+0.92	-0.04	9.3	341	+28	Classified E in (1).
2300-18	(3)	445	17.82	+0.62	-0.19	10.0	46	-64	Redshift by Searle and Bolton (1968).
		447	17.78	+0.66	-0.09				

TABLE III. PHOTOMETRY OF RADIO GALAXIES

Parkes Catalogue Number	NGC	Finding Chart	Type	V	B-V	U-B	Aperture in seconds of arc
0036+03	193	included	E2	12.95	+1.04	+0.48	*39
0123-01	545/7	(12)	db	11.88	1.05	0.54	*80
0131-36		(14)	SOp	13.24	1.02	0.50	83
				13.78	1.01	0.41	36
0153+05	741/2		EO/E	12.63	1.04	0.70	39
0238+08	1044		db	13.27	1.22	0.57	80
0240-00	1068		SAb(rs)(R)	8.98	0.72	0.08	*286
				9.64	0.74	0.02	80
				10.02	0.78	0.04	39
				10.56	0.83	0.06	20
				11.05	0.87	0.06	11.6
				11.63	0.82	0.06	7.0
0255+05		(12)	db	13.16	1.16	0.80	80
0305+03	1218	(12)	SO	12.94	1.17	0.76	80
0320-37	1316		SAB(s)Op	9.14	0.92	0.50	*180
				9.30	0.92	0.52	136
				9.58	0.94	0.54	91
				9.92	0.97	0.56	59
				10.37	0.96	0.58	37
				10.60	0.97	0.60	30
				11.17	0.97	0.64	18.2
				11.81	1.00	0.67	8.3
				13.10	1.13	0.74	5.0

Parkes Catalogue Number	m_r	l_{II}	b_{II}	Redshift corr. for galactic rotation km/sec	Remarks
0036+03	9.4	117^o	-59^o	4350 (17)	4C 03.1
0123-01	8.1	142	-63	5390 (12)	3C 40.
0131-36	7.8	261	-77	8930 (16)	R.
0153+05	9.9	153	-53	5640	4C 05. 10; R.
0238+08	9.7	163	-45		4C 08.11
0240-00	9.0	172	-52	1090	3C 71; R.
0255+05	8.0	170	-45	7240 (12)	3C 75; R.
0305+03	8.5	175	-45	8670 (13)	3C 78; R.
0320-37	4.9	239	-57	1715	Fornax A; R.

Parkes Catalogue Number	NGC	Finding Chart	Type	V	B-V	U-B
0449-17		(5)	E	13.65	+0.98	+0.56
0427-53	IC2082	(14)	db	13.20	1.15	0.82
				13.69	1.08	0.52
0722-09		(4)	Sc	14.89	1.06	0.30
0833-01		(5)	E	12.66	1.00	0.50
0843-33	2663		E3	12.33	1.26	0.90
				12.98	1.26	1.09
				13.78	1.38	0.93
0915-11		(3)	db	13.65	1.07	0.46
1116-46			E	15.30	1.10	0.53
1123-35		(1)	E3	13.85	1.15	0.77
1142+19	3862		E0	13.13	1.03	0.66
1216+06	4261		E2-3	10.82	0.95	0.53
1222+13	4374		$E^{+}1$	9.73	1.00	0.66
				9.91	0.99	0.62
				10.15	1.00	0.61
				10.45	1.01	0.61
				10.85	1.01	0.66
				11.02	1.02	0.68
				11.74	1.06	0.67
				12.31	1.11	0.71

Parkes Catalogue Number	Aperture in seconds of arc.	m_r	l_{II}	b_{II}	Redshift corr. for galactic rotation (km/sec.)	Remarks
0449-17	59	9.1	216°	-34°		R
0427-53	55	8.4	262	-42	11750(16)	R
	36					
0722-09	*18.2	11.9	225	+2	2190(7)	3C178;R.
0833-01	83	10.3	227	+22		
0843-33	36	9.1	256	+6		R
	18.2					
	9.2					
0915-11	80	5.8	243	+25	15650(12)	Hydra A; R.
1116-46	18.2	8.5	287	+13		
1123-35	22.6	8.9	284	+24		
1142+19	59	8.0	236	+73	6180(13)	3C264;R.
1216+06	*136	7.3	282	+67	2090	3C270;R.
1222+13	*180	8.3	278	+74	878	3C272.1;R.
	136					
	91					
	59					
	37					
	30					
	15.2					
	8.3					

Parkes Catalogue Number	NGC	Finding Chart	Type	V	B-V	U-B
1228+12	4486		EO-I_p	9.50	+1.01	+0.62
				9.65	0.99	0.63
				9.98	1.02	0.66:
				10.32	1.01	0.63
				10.82	0.99	0.63
				11.07	1.01	0.61
				12.08	1.05	
				12.86	1.07	0.64
1245-41	4696		E1	11.46	1.02	0.64
				12.43	1.04	0.75
1252-12	4782/3		E^+O_p/EO_p	11.15	1.01	0.61
	4782			12.54	1.05	0.69
	4783			12.78	0.99	0.63
1332-33	IC4296		EO	11.11	1.03	0.61
				11.20	1.02	0.62
				11.53	1.04	0.62
				11.71	1.03	0.64
				12.08	1.02	0.61
				12.51	1.06	0.65
				12.74	1.08	0.68
1334-29	5236		SAB(s)c	8.77	0.69	-0.07
				10.02	0.73	-0.11
				10.52	0.73	-0.25
				10.97	0.49	-0.37
				11.40	0.37	-0.37
1400-33	5419		EO	11.60	1.05	0.77
1407-17	5490		E2-3	12.35	1.03	0.52

Parkes Catalogue Number	Apertures in seconds of arc.	m_r	l_{II}	b_{II}	Redshift corr. for galactic rotation (km/sec)	Remarks
1228+12	*180	3.9	204°	+74°	1190	Virgo A; R.
	136					
	91					
	59					
	37					
	30					
	15.2					
	8.3					
1245-41	* 91	8.1	302	+22	2570	R.
	37					
1252-12	*136	7.5	304	+50		3C278; R.
	* 30				3860	
	* 30				4530	
1332-33	*136	7.2	313	+28	3430(15)	R.
	110					
	83					
	55					
	36					
	22.6					
	18.2					
1334-29	*286	8.4	315	+32	335	R.
	80					
	39					
	20					
	11.6					
1440-33	*80	8.0	320	+27		R.

Parkes Catalogue Number	NGC	Finding Chart	Type	V	B-V	U-B	Aperture in seconds of arc	m_r	l_{II}	b_{II}	Redshift corr. for galactic rotation (km/sec)	Remarks
1414+11	5532		E2	12.15	1.07	0.57	*55.4	8.7	358	+64	7110	4C10.39;R.
1416-49			E	16.23	1.29	0.48	18.2	8.9	317	+11		
1610-60		included	E	12.83	1.21	0.74	*39	6.4	325	-7		R
1834+19		included	E	13.53	1.12	1.04	*39	9.3	49	+12		R
2040-26		(1)	E	13.52	0.52	0.04	*22.6	8.9	19	-35		R
2058-28		(1)	E	14.75	1.16	0.76	22.6	7.8	18	-39		R
2152-69		(14)	D or E	13.79	0.99	0.21	39.0	6.2	322	-41	7980(15)	R
2212+13	7236/7		db	12.98	1.05	0.44	*80	8.1	75	-34	8095	3C442;R.
2247+11	7385		EO	12.66	1.08	0.47	80	8.5	82	-41	8050	
2308+07		included	E	13.59	1.12	0.45	80	8.8	84	-48		4C07.61;R.
2318+07	7626		E1	11.80	1.04	0.60	*80	10.1	88	-48	3550	
2354-35		(1)	D	14.36	0.97	0.59	22.6	8.5	356	-76		

REMARKS to TABLE III.

01 31 - 36. — Optical features described in (14). — Interferometry at 470 and 1400 MHz indicates a double source, separation 8' long P.A. 90°, components 3.5' x 2.5'; additional structure present in the components (8).

0153 +05. — UBV measures are of NGC 741 only which is the brighter of the two.

0240 - 00. — Seyfert galaxy, bright nucleus, faint surrounding ring. Structure discussed recently by Walker (1968). — Core-halo type radio source, centred on nucleus. Some evidence of scintillation, i.e. small fraction of emission is from a region 1" in diameter, possibly the nucleus.

0255 +05. — Two EO galaxies, in loose cluster Abell 400 (Abell 1958) — At 960 MHz, source is double, components equal in intensity dia. 1.2', separation 2.8' along P. A. 47°.

0305 +03. — In Perseus cluster. — Roughly circular at 960 MHz.

0320 -37. — Either 6583 [N II] or H$_\alpha$ present in emission. Faint optical extensions connecting each radio emitting region to galaxy. Axis of rotation along minor axis, perpendicular to plane of these extensions. (Searle 1965). — At 300 MHz, source is double. Component intensity radio is $\sim$1.9:1, diameters each 18', separation 29' along P. A. 100°. Components skewed, suggesting additional structure.

0449 -17. — UBV measures include faint field star.

0427 -53. — Optical structure in (14). See also Sersic (1961). Bright star included in UBV measures.

0722 -09. — Small bright nucleus. Small aperture used because of crowded field. At 960 MHz, d$\lesssim$1!0 NS

0843 -33. — Colours reddened by galactic absorption. — Interferometry at 470 and 1400 MHz indicates core-halo type of source, 4'x 2', extended along P. A. 170^{o} (8).

0915 -11. — Brighter member has two nuclei in a common envelope. — At 960 MHz, source has halo with d$\sim$5' (12% of flux) , and non circular core, 1.2' in P. A. 30^{o} and d $\lesssim$0.6' in P. A. 90^{o} and 150^{o}. Core has d = 42" at 1420 MHz and unresolved companion.

1142 +19. — In cluster Abell 1367. — At 960 MHz, source has halo with d$\gtrsim$6!0, and core of d 1!2 having 60 percent of flux.

1216 +06. — Optical size 1!6 x 1!3. — At 960 MHz, source has two components of equal intensity each d = 2.7', separation 4.7' along P. A. 85^{o}.

1222 +13. — M84, in Virgo cluster. Optical size 2!9 x 2!6. — At 178 MHz d = 4!2; at 960 MHz d = 1!8 NS.

1228 +12. — M87 in Virgo cluster. Very massive. The well known jet extends 18" from the bright nucleus (PA 290^{o}) and emits optical synchrotron radiation. Strong λ3727 [O II] indicates presence of ionized gas in nucleus. The velocity profile indicates an component in the gas expanding at 900km/sec. Large number of surrounding globular clusters. — A core-halo source. At 1420 MHz the core consists of two components each having d = 23^{o}", with EW separation of 31" along P. A. 285". The eastern component probably coincides with the jet. The halo distribution has a diameter of 6.5' or 30 kpc.

1245 -41. — Optical size 1.7' x 1.2'. Measurement with 95" aperture possibly includes a field star. d $\lesssim$ 15" at 86 MHz.

1252 -12. — Both components massive, 4783 less condensed. No emission lines detected. At 159 MHz 47" $\lesssim$ d $<$ 4'. At 960 MHz, source roughly circular, d = 2.2'.

1332 -33. — Appears at 2650 MHz as a three component source, component B (7.4' x 7.6') coinciding with the galaxy. (Cf. Gardner and Davies 1964).

1334 -29. — Optical size 10' x 8'. Large amount of dust in the system. Emission lines observed in nucleus. — Interferometry at 470 and 1400 MHz indicates a core-halo type of source, Halo 7' x 7', core $\lesssim$1' in diameter. Halo/core flux ratio 9:1 (8).

1400 -33. — Optical size 1' x 0'.7. — At 86 MHz d $\gtrsim$ 45".

1414 +11. — Curved spectrum.

1610 -60. — UBV colours reddened by galactic absorption. — A double source at 2650 MHz. The stronger component shows multiple-component structure from interferometry at 470 and 1400 MHz. The galaxy is at the centroid of the strong component; the weaker component may not be physically related (8).

1834 +19. — UBV colours reddened by galactic absorption.

2040 -26. — Interferometry at 470 and 1400 MHz indicates a double source, components each 2.0' x 0.9', separated by 3.0' along P.A. 157°(8).

2058 -28. — Interferometry at 470 and 1400 MHz indicates a double source, components each 1.5' x 1.3', separated by 2.8' along P.A. 155°(8).

2152 -69. — Interferometry at 470 and 1400 MHz indicates a double source, components 2.0' x 0.5' and $\lesssim$1.0', separated by 3.8' along P. A. 96°. Component intensity ratio is 7:1, and the weaker component has a flatter spectrum. Stronger component centred on galaxy; the weaker may hence be not physically associated (8).

2212 +13. — SO galaxies with bright nuclear regions separated by 40" in a common envelope. — At 178 MHz, $4' < d < 10'$, At 960 MHz, d = 3.0' NS.

2308 +07. — One of three central bright galaxies of cluster Abell 2551. At 1410 MHz, $d < 6'$.

References to Tables I, II and III.

(1) Bolton, J. G., Clarke, Margaret E. and Ekers, R. D. 1965.

(2) Bolton, J. G. and Ekers, Jennifer 1966a.

(3) Bolton, J. G. and Ekers, Jennifer 1966b.

(4) Bolton, J. G. and Ekers, Jennifer 1966c.

(5) Bolton, J. G. and Ekers, Jennifer 1967.

(6) Bolton, J. G. and Kinman, T. D. 1966.

(7) Burbidge, E. M. 1967.

(8) Ekers, R. D. 1967.

(9) Ekers, R. D. and Bolton, J. G. 1965.

(10) Kinman, T. D., Bolton, J. G., Clarke, R. W. and Sandage A. 1967.

(11) Kinman, T. D. and Burbidge, E. M. 1967.

(12) Maltby, P., Matthews, T. A., and Moffet, A. T. 1963.

(13) Schmidt, M. 1965.

(14) Westerlund, B. E. and Smith, Lindsey, F. 1966.

(15) Westerlund, B. E. and Stokes, N. R. 1966.

(16) Westerlund, B. E. and Stokes, N. R. 1968.

(17) Wills, D. 1967.

TABLE IV. PHOTOMETRY OF NORMAL GALAXIES

Object	Type	V	B-V	U-B	Aperture in sec. of arc.	l_{II}	b_{II}	Redshift corr. for gal. rot. km/sec.	Remarks
Anon., near 0036+03	E	13.06	+0.92	+0.52	80	117°	-59°		7' NW of 0036+03
NGC 541	E	12.72	+0.98	+0.47	80	142	-63		Connected to NGC 545/7 (0123-01) by a faint, bridge
Anon., near 0131-36	E	13.25	+1.04	+0.55	55	261	-77		At $01^h33.^m9$, $-36^o.'9$ (1950)
NGC 1947	SO^-p	11.15	+1.05	+0.66	110	273	-33		Dark lanes
		11.66	+1.04	+0.52	55			930	
		12.79	+1.09	+0.66	22.6				
NGC 3955	IO	12.12	+0.66	+0.03	110	286	-38	1310	Bright knote & dark lanes. See Hodge (1966), Tovmassian (1966).
		12.50	+0.65	+0.12	55				
		12.83	+0.65	-0.03	36				
		13.33	+0.64	-0.15	22.6				
		13.69	+0.58	-0.11	18.2				
		15.00	+0.84	+0.04	9.2				
NGC 4264	S(rs)0	13.22	+0.94	+0.59	37	282	+67		Near NGC 4261 (1216+06)
NGC 4406	E^+3	9.92	+0.93	+0.57	180	279	+75	-367	Near M84 (1222+13)
NGC 4478	2	11.56	+8.87	+0.57	136	284	+74	1410	Near M87 (1228+12)
IC 4662	In	11.52	+0.40	-0.33	110	329	-18		Dominated by two large HII regions.
Anon., near IC 4296	S	12.75	+1.04	+0.54	110	314	+28		Very bright nucleus; spiral structure extremely faint. 5'.6 S of IC 4296, at $13^h33.^m7$, $-33^o48'$ (1950).
		13.23	+1.05	+0.67	36				
		13.77	+1.04	+0.68	18.2				
NGC 6930	SB1	12.07	+0.87	+0.40	110	204	-22	4550	Interacting with IC 4970

Object	Type	V	B-V	U-B	Aperture in sec. of arc.	l II	b II	Redshift corr. for gal. rot. km/sec.	Remarks
		12.45	+0.99	+0.71	55				
		13.36	+1.03	+0.69	22.6				
		14.00	+1.00	+0.66	18.2				
		14.44	+1.07	+0.76	9.2				
NGC 6876	E3	12.47	+1.03	+0.54	36	324	-33	3580	Field star may affect 34" dia. measure.
		12.93	+1.02	+0.74	22.6				
		13.55	+1.03	+0.67	18.2				
IC 4970	SAO$^-$	13.93	+0.83	+0.38	36	324	-33		
		14.20	+0.78	+0.32	22.6				
		14.91	+0.69	+0.33	18.2				
NGC 6877	E6	13.48	+1.13	+0.54	36	324	-33		
NGC 7232	SB(rs) a	13.73	+0.55	-0.31	22.6	351	-54	1860	Inner ring has dim. 0.'55x0'.1
		13.98	+0.57	-0.29	18.2				
		14.78	+0.51	-0.28	9.2				
NGC 7386	SO	12.90	+1.09	+0.47	80	82	-41	7420	Near NGC 7385 (2247+11)
Anon., (a) near 2308+07	E	13.61	+1.22	+0.34	80	84	-48		Faint spiral galaxy incl. in U, B, V measures.
Anon., (b) near 2308+07	E	13.36	+1.02	+0.55	80	84	-48		
NGC 7619	E3	11.76	+1.05	+0.62	80	88	-48	3954	Near NGC 7626 (2318+07)

TABLE V. DATA FOR SOME RADIO GALAXIES AND FOR RADIOQUIET GALAXIES IN THEIR IMMEDIATE NEIGHBORHOOD

PARKES CATALOGUE NUMBER	NGC	V	B-V	U-B	SEPARATION	TYPE
0036+03	-	12.95	1.04	0.48	7.0'	E2
	-	13.06	0.92	0.52		E
0123-01	545/7	11.88	1.05	0.54	5.0'	E,E
	541	12.72	0.99	0.47		E
1216+06	4261	10.82	0.95	0.53	3.5'	E2-3
	4264	13.22	0.94	0.59		S(rs)0
1222+13	4374	9.73	1.00	0.66	17.0'	E^+1
	4406	9.92	0.93	0.57		E^+3
1228+12	4486	9.50	1.01	0.62	9.0'	E0
	4478	11.56	0.87	0.57		E2
2247+11	7385	12.66	1.08	0.47	6.0'	E0
	7386	12.90	1.09	0.47		S0
2308+07	-	13.59	1.12	0.45	3.0'	E
	-	13.61	1.22	0.34	5.0'	E
	-	13.36	1.02	0.57		E
2318+07	7626	11.80	1.04	0.60	7.5'	E1
	7619	11.76	1.05	0.62		E3

TABLE VI.

ADDITIONAL OBJECTS PLOTTED IN FIG. 5.

a. THE QSO:s IN AIZU et al's CATALOGUE

OBJECT	M_{158}	$m_{158}-m_{pg}$
3C47	-35	-10
3C48	-35	-9
3C147	-38	-11
3C273B	-30.8	-4
3C286	-38	-9

b. Radio Sources in Searle and Bolton's list.

OBJECT	Type	M_{158}	$m_{158}-m_{pg}$
0115+02	QSO	-32.0	-7.4
0159-11	QSO	-32.7	-8.1
0349-27	E	-28.6	-8.3
1004+13	QSO	-29.9	-5.8
1131+21	E	-26.7	-5.7
1358-11	E	-25.3	-5.1
1514+00	E	-29.7	-6.5
2128-12	QSO	-29.5	-3.6
2134+04	QSO	-31.1	-4.7
2349-01	N	-29.2	-7.5

c.

OBJECT	TYPE	M_{158}	$m_{158}-m_{pg}$
3C120	Seyfert	-26.8	-6.3
3C171	N	-26.8	-5.4

TABLE VII.

SAMPLES OF ARP'S GROUPS OF OBJECTS

Arp No.	QSO	Radiogalaxy or unknown	No. of central galaxies	$M_r - m_{pg}$	M_r
148	3C254 3C247	3C252	1	-6.8	-27.6
	3C254			-9.3	-33.6
139,196	3C287	3C277.3 3C284	2	-6.7	-29.7
	3C287			-7.5	-32.2
134	3C273	3C274	1	-4.0	-25.9
	3C2736			-4.0	-30.8
NGC5223	3C286	3C288	3	-6.0	-26.0
	3C286			-9.0	-38.0
130					
	3C9			-6.5	-32.4
35,201					
	3C2			-8.5	-31.5
NGC4651	3C275.1		1	-3.2	-23.2
	3C275.1			-10.7	-33.4

TABLE VIII. SURFACE BRIGHTNESS DISTRIBUTIONS (Mag / □") AND COLORS DISTRIBUTIONS

(a) NGC 4374

A_B = 0.40 ; D = 1.

S_v	B-V	U-B	r"
21.87	+1.06	+0.91	79.8
21.45	.95	.66	57.8
20.64	.97	.61	38
19.78	1.01	.50	24.7
19.37	.95	.56	16.9
18.61	1.00	.67	11.9
17.93	.99	.63	6.1
16.65	1.11	.71	3.0

(b) NGC 4486

A_B = 0.40 D = 1.

S_v	B-V	U-B	r"
21.82	+1.11	+0.59	79.8
20.87	.92	.55:	57.8
20.36	1.04	.75:	38.3
19.45	1.04	.63	24.7
18.98	.90	72	16.9
18.42	.99	61	11.9
18.03	1.03	60	6.1
17.20	1.07	64	3.0

(c) IC 4296

A_B = 1.1 D = 2.95.

S_v	B-V	U-B	r"
23.14	+1.17	+0.47	61.5
21.69	.97	.62	48.3*
22.28	1.11	.49	34.5
20.90	1.06	.71	22.8
20.28	.93	.54	14.7
19.71	.98	.53	10.2
18.78	1.08	.68	6.5

* Data in this zone disturbed by bright star.

(d) NGC 1316

A_B = 0.60 D = 1.43.

S_v	B-V	U-B	r"
21.41	+0.92	+0.36	79.8
20.68	.85	.46	57.8
19.96	.86	.49	38.3
19.14	.99	.52	24.7
18.61	.92	.42	16.9
18.20	.97	.59	12.4
17.84	.93	.61	7.1
16.05	.95	.65	3.5
16.33	1.13	.74	1.8

(e) NGC 1068

A_B = 0.80 D = 0.91.

S_v	B-V	U-B	r"
21.77	+0.69	+0.16	92
19.93	.65	- .03	29.5
18.40	.70	+ .02	15
17.45	.77	+ .06	7.9
16.58	.94	06	4.7
15.60	.82	.06	1.8

(f) NGC 5236

A_B = 1.0 D = 0.58.

S_v	B-V	U-B	r"
21.11	+0.67	-0.04	92
20.06	.73	+ .20	29.5
19.05	1.47	.11	15
17.99	.80	- .38	7.9
16.46	.37	- .37	2.9

(g) NGC 6872

$A_B = 0.93$ D = 3.80.

S_v	B-V	U-B	r"
23.05	+0.60	+0.05	41.3
21.30	.96	.73	21.0
19.62	1.07	.73	10.2
20.91	.87	.52	6.9
19.00	1.07	.76	2.3

(h) NGC 3955

$A_B = 0.82$ D = 1.09.

S_v	B-V	U-B	r"
23.08	+0.69	-0.18	41.3
21.79	.65	+0.70	22.8
20.89	.67	+ .23	14.7
20.10	.80	- .27	10.2
19.80	.48	- .16	6.9
19.56	.84	+ .04	2.3

(i) NGC 7232

A_B = 0.63 D = 0.63.

S_v	B-V	U-B	r"
20.85	+0.46	-0.38	10.2
20.41	0.62	-0.30	6.9
19.34	0.51	-0.28	2.3

(j) NGC 1947

A_B = 0.90 D = 0.78.

S_v	B-V	U-B	r"
21.84	+1.07	+0.97	41.3
20.38	1.01	0.45	21.0
19.30	1.09	0.66	16.0